LA-UR-94- 4316

Title: Real-Time Monitoring of Alpha Emissions

Author(s): Russ Gritzo, Malcolm Fowler, and Jan Wouters

Submitted to: FISCAL YEAR 1994 FINAL REPORT

Los Alamos
NATIONAL LABORATORY

Form No. 836 R5
ST 2629 10/91

Los Alamos National Laboratory

Real-Time Monitoring of Alpha Emissions

TTP AL142003

Fiscal Year 1994 Final Report

R. Gritzo, M. Fowler, J. Wouters

Table of Contents

Introduction

Abstract

This is the fiscal year 1994 final report for TTP AL142003, Real-Time Monitoring of Alpha Emissions.

Los Alamos National Laboratory (LANL) is developing a technology for on-line, real-time monitoring of incinerator stacks for low levels of airborne alpha activity. Referred to as the Large-Volume Flow Thru Detector System (LVFTDS), this technology uses a unique design for sensitive, real-time measurements of alpha particle emissions. This technology directly addresses the public's demand for fast responding, high sensitivity effluent monitoring systems.

This past year's effort was built on the proof of concept demonstration from the previous year, taking the detector development one step closer to field trials. Toward this end three primary goals were reached:

- The detector background was reduced by as much as a factor of 50 in some configurations.
- A second generation detector, twice the size of the original unit, was built and tested.
- The detection sensitivity estimated in the beginning of the project was reached and demonstrated by monitoring ambient levels of radon in normal room air.

This final report is a compilation of accomplishments in background reduction, once-through flow testing, and aeronautical and mechanical engineering.

Background

This effort began in fiscal year 1992, when Los Alamos National Laboratory (LANL), then group INC-13, was asked to survey the state of the art of real-time alpha monitoring technology that was used in stacks or could easily be adapted for use in stacks. The primary motivation was the understanding that public opposition was one of the major factors preventing the building and operation of nearly all mixed and low-level waste incinerators. Much of this opposition was based on a lack of continuous real time monitoring of the stacks. With incineration being one of the best available treatments of much of the mixed and low level waste, and a lack of real-time monitoring hampering incinerator permitting, real-time emissions monitoring became a key requirement in the treatment of mixed and low-level waste.

Fiscal Year 1992

In fiscal year 1992 a detailed survey of commercial alpha monitoring technology was performed by LANL [1]. We found that, with some minor variations, nearly all commercial alpha monitoring techniques are based on a common approach, consisting of extracting a sample of the gas being monitored and passing it through a filter placed close to a detector sensitive to alpha decay radiation. Particulates bearing alpha emitting radionuclides are entrained on the filter and subsequent alpha decays are measured by the detection system.

This approach, while useful in many applications, is inherently an integrating technique and not well suited to real-time applications. Additionally, the small volume of gas measured is assumed to be representative of the remainder of the stack. Sampling a relatively small fraction of the total flow in the stack limits the useful sensitivity of the instrument.

With these limitations in mind, Los Alamos then began evaluating other possible alpha monitoring technologies. Based on concepts being developed for a different application, we proposed the development of a new monitoring technology.

This new technology uses multiple parallel plates of scintillating material fabricated such that the entire stack gas stream flows directly through the inter-plate volume. Light from the scintillations produced by the alpha particles striking the plates is collected and processed to determine the concentration of alpha emitting radionuclides present in the air.

Enough experimental work was done in FY 92 to establish a basis for some performance estimates of a detector built from this new technology. These estimates were quite promising, indicating the potential for more than an order of magnitude improvement in sensitivity at short integration times. A proposal was written and funded for development of the technology up to a lab-scale prototype for Fiscal Year 93 [2].

Fiscal Year 1993

The lab scale prototype detector designed in FY93 allowed us to demonstrate the proof of concept using a radioactive gas. This was done on a scale large enough to effectively demonstrate the concept, but small enough to be easily constructed, handled, and altered as needed. This prototype detector consisted of 5 scintillator plates forming a 10 liter active volume detector. While small by our original performance estimates, a detector of this size would fit comfortably in the 25 cm (~10") diameter stacks of some thermal treatment systems.

A number of closed-loop tests were conducted in which radon was introduced into the detector box for a short time and then stopped. We continued to re-circulate the air in the box while the contained radon decayed. Out of this series of tests we were able to reach the following conclusions:

- The detector concept was sound.
- We were able to easily detect concentrations of alpha emitting radionuclides in air at a few hundred picoCuries per liter in real time with short (5 second) latency.
- We measured a volumetric detection efficiency of ~73%, in close agreement with our predicted efficiency of 75%.
- The performance was stable over long periods of time.

Amongst all this success, we found that the background in the detector was higher than we had hoped for, based on the early work we had done. This high background was the main factor limiting the sensitivity. Plans were made for the following fiscal year to better characterize the background, conduct experiments investigating the nature of the background, and to determine approaches for significant background reduction.

In concert with the technical development, market research was conducted, an industry workshop showcasing the technology was held, and an industrial partner, EG&G Nuclear Instruments, was selected. More detail can be found in the FY 93 Final Report [3].

Fiscal Year 1994

In Fiscal Year 1994, the program was transferred to the Mixed Waste Integrated Program (MWIP) and funded under TTP AL142003. The goal of the program in FY 94 was to take the development of the detector to an intermediate level, between the lab scale prototype of FY 93 and the full scale demonstration planned for late FY 95. Along the way three main subjects were to be addressed: background reduction, once-through flow tests, and aeronautical and mechanical engineering.

In the sections that follow each of these topics are introduced and the work performed in the past fiscal year summarized.

FY 1994 Final Report

This fiscal year final report is largely a compilation of three separate reports detailing the background reduction, the once through flow tests, and the aeronautical engineering work. The full text of each report is included as an appendix to this report.

In the final section the plans for FY 95 are outlined.

References

[1] Incinerator Off-Gas Containment and Analysis Tasks (LATO-EG&G-91-012, EG&G P.O. 98662GD) Subtask 2a Final Report, Los Alamos National Laboratory, currently in preparation for publication, copy available from R. Gritzo upon request.

[2] Gritzo, R., TTP AL121218, LANL Support for EG&G/RF/NMWP Real-Time Emission Monitoring, Los Alamos National Laboratory, Revision 2, March 26, 1993.

[3] Gritzo, R. et.al., Los Alamos National Laboratory Support for EG&G Rocky Flats National Mixed Waste Program Real Time Emission Monitoring, Final Report, Los Alamos National Laboratory, currently in preparation for publication, copy available from R. Gritzo upon request.

Background Reduction

Introduction

As with virtually any radiation detection system the background coming from naturally occurring radioactive processes places one of the most significant limits on the ultimate sensitivity achievable. Our earlier work demonstrated clearly that the detector concept was sound, but that the measured backgrounds were significantly reducing our expected sensitivity. As a result, we implemented a program in FY 94 to evaluate three separate approaches for reducing the detector background.

Passive Shielding

One strategy was to simply add a high density material such as lead or steel around the detector to attenuate external sources of radiation. Since the scintillator plates were deliberately made as thin as possible they already had a low efficiency for penetrating forms of radiation (such as gamma rays). Adding passive shielding would primarily reduce the low energy component of the observed background.

Plate Multiplicity Veto

The next strategy was to make use of the multiple elements of the detector to reduce the detected background in the following manner. Alpha particles have only a very short range; thus an alpha particle will strike only one plate. More penetrating radiation (such as high energy cosmic rays, gamma rays, etc) will strike more than one plate, essentially simultaneously. Thus any detected signal that fires two or more plates within some narrow time window cannot be due to an alpha particle and may be eliminated.

Energy Discrimination

Finally, the particular plate design we chose has a high enough light production and transport efficiency that we are able to roughly determine of the amount of energy deposited in the plate by any given event. While we are not able to tell, say a 5.5 MeV alpha from a 4.9 MeV alpha, we can certainly tell the difference between an alpha particle and a high energy beta or gamma ray. By adjusting the data acquisition system to accept only signals large enough to have a high probability of being an alpha event, an additional background reduction can be achieved.

Research Report

Each of the three strategies for reducing the background outlined above were researched in considerable detail. A thorough summary of the work has been completed as a separate document. A copy of this paper is attached as appendix A.

Summary

The results of this effort indicate that a combination of all three techniques suppresses the detected background by more than an order of magnitude, without significantly affecting the alpha detection efficiency.

This portion of the FY94 program was highly successful, achieving background reduction factors as high as 50. This reduction translates into an improvement in the overall detector sensitivity of a factor of 7. In practice, though, we did not expect to achieve a background reduction factor of more than 25 to 30 since the conditions in the full detector assembly were deemed to be poorer for background reduction than that of the optimized test assemblies.

Using the results of this study, we implemented all the background reduction measures in the detector being used for the once through flow tests (see next section). Our preliminary results indicate that a background reduction factor of almost 40 has been achieved.

This result is significant because we have achieved an average background for an operational detector almost a factor of two better than we had predicted (0.65 cpm/in^2 vs 1.0 cpm/in^2). Although we have reduced the detection efficiency somewhat by removing the 1 pe peak from the plate spectrum, combining these two effects brings the overall detector sensitivity to levels at or slightly better than our original estimates.

Once-Through Flow Tests

Introduction

The Fiscal Year 1993 detector demonstration was conducted using a closed-loop, recirculating configuration. This very successful test allowed us to clearly demonstrate the operational principles of the detector and measure the alpha detection efficiency. The primary thrust of the FY 94 effort was to bring the overall system one step closer to field application. Part of this effort was reconfiguring the system such that room air was pulled through the detector in a single pass.

This single pass, or once through flow setup, offered opportunities to advance the development in several areas:

- Increase the Active Volume. The original prototype had a 10 liter active volume, while the once through flow setup was twice the size at 20 liters. The unit being designed for field testing will have an active volume of nearly 28 liters.
- Measure Low Levels of Activity. Radon is a naturally occurring radioactive gas, present in room air at the few picoCuries per liter level. This setup, using the background reduction techniques being developed, gave us experience in detecting low levels of airborne activity.
- Testing Long Term Stability. This configuration allowed us to run the detector and data acquisition system continuously for extended periods of time (several weeks) and evaluate the long term stability of the various elements.
- Data Acquisition System Development. Doubling the size of the detector (by doubling the number of plates) required us to develop a new approach to

acquiring data from the system. Several improvements were made in the speed at which events were processed and archived.

- Develop Light Tight Configurations. Since the detector photomultiplier tubes operate in the single photoelectron counting regime ensuring that no stray light enters the detector enclosure is critical.

Research Report

A report detailing the mechanical configuration of the detector was prepared by one of the project summer students, Chris Darr. A copy of the report is included as Appendix B.

Summary

A number of tests have been run using room air, making a single pass through the detector. The detector data clearly shows both short term (10s of minutes) and long term (several hours) fluctuations in ambient radon and radon daughter product levels.

The development of a full understanding of the data taken is a difficult task. Variations in the low levels (~1 to 2 pCi/liter) of naturally occurring radon, uncertainty and fluctuations in the fate of the radon daughters, and the complexity of a lengthy decay chain complicate the data analysis.

We are currently conducting more detailed analysis of the data, and are planning a new series of tests using a controlled radon source. We expect results of those tests in the second quarter of FY 95.

Aeronautical and Mechanical Engineering

Introduction

The LVFTDS concept requires the detector elements to operate while inserted directly in the full effluent flow of the system being monitored. Although proper functionality is not contingent upon maintaining specific flow characteristics, certain aerodynamic issues must be addressed. These include pressure drop calculations and measurements, fluid flow modeling and visualization, and mechanical design of the plates (including the leading edge).

The bulk of this work was subcontracted out to Arizona State University (ASU) as part of the FY 94 project. A LANL summer student, Chris Martinez, performed much of the work under the direction of the ASU researchers. Chris is currently an undergraduate student in the Aeronautical and Mechanical Engineering Department at ASU.

A summary of the issues being addressed under this subcontract is provided below.

- Create a control-volume model of the detector system for fluid-dynamic analysis.
- Perform analysis to predict pressure drop as a function of flow parameters.
- Perform tensile testing to determine the modulus of the scintillator material.
- Select a suitable surrogate material for mechanical testing and fabricate a test article and supporting structure.
- Create a finite-element model of the detector system for dynamic and structural analysis.

- Conduct flow visualization experiments.
- Measure the pressure drop and vibrational response under different flow conditions.

The duration of the contract and completion of these tasks was expected to be 7 months.

Research Report

A copy of the preliminary report summarizing the fluid flow modeling effort, prepared by Chris Martinez (LANL Summer UGS and Arizona State University Student) is included as appendix C. This is a draft version of the report. The final version had not been completed at the time of this writing.

Summary

Effort under this subcontract was not started until June of 94 and so only a portion of the work was completed prior to the end of FY94.

Models were designed and code written to perform both dimensional and non-dimensional analysis on a detecting cell. Use of these models indicated that over a wide range of fluid viscosities (temperatures) and flow rates a transition from laminar to turbulent flow was expected within the detector. Fortunately, in most incinerator off gas systems the flow is assumed to be turbulent, and special steps must be taken to create a laminar flow section. The decision was made to require turbulent flow through the detector volume, and so no corrective action to eliminate a possible laminar to turbulent transition region was deemed necessary.

This conclusion eases the installation concerns. Since laminar flow is not needed, and in fact is not wanted, both the detector piping and the plates themselves can be much simpler. Although final numbers were not available at the time of this report, initial pressure drop and plate element forces were expected to be quite low.

Summary

Fiscal Year 94 - Looking Back

A number of important accomplishments were achieved in Fiscal Year 1994, bringing the detector development one step closer to field trials. These achievements include:

- Building and testing a second generation detector, twice the size of the original unit.
- Reaching the detection sensitivity estimated at the beginning of the project and demonstrating this achievement by monitoring ambient levels of radon in normal room air.
- Achieving significant reductions in detector background, in some configurations by as much as a factor of 50.
- Commitment for industrial partnering with EG&G Nuclear Instruments.

Other Fiscal Year highlights include:

- Presentation of the detector technology at the 1994 International Incineration Conference.
- Subcontract with Arizona State University
- Collaboration with students from 3 major Universities, including a Minority Engineering program.
- Kept ourselves off the streets and out of the bars.

Fiscal Year 95 - Looking Ahead

All of the past years' work has been focused on one long term goal; successful field demonstration. The first of these demonstrations is planned for FY 95.

We have selected the Incineration Research Facility in Arkansas as the most suitable site for the initial field tests. We are currently making the design modifications for the detector system to be used for this test.

Testing is planned for June 1995, and will consist of three phases. The functional test phase, the first of the three, will verify the detector background and alpha detection performance under nominal conditions. The second phase will consist of a series of challenges such as temperature and humidity excursions. The final phase will consist of long-term exposure of the detector to the off-gas environment for life-cycle testing.

At the close of FY 95 we plan to have successfully field tested and documented the system performance in anticipation of installation at a treatment facility.

Appendices

Appendix A

Sensitivity Enhancement of the Large Volume Flow Through Detector

Los Alamos National Laboratory

14. December, 1994

Sensitivity Enhancement of the Large Volume Flow Through Detector

Christopher J. Darr
Joel E. Farnham
Jan M. Wouters

Introduction

To dispose of the radioactive waste products that have been or are being created by government agencies and private companies, the Department of Energy is developing thermal treatment techniques to greatly reduce the waste volume. As part of this effort, several detector systems are under development to monitor the effluent of treatment systems and thus guard against the inadvertent release of hazardous and/or radioactive materials to the environment. We are developing such a detector – an on-line, real time monitor for alpha emitting nuclides that can detect low levels of Pu, Am, and similar nuclides which could be present in a gaseous waste stream.

The key to the detection of low-levels of any radionuclide is to minimize all background signals that may interfere with the signal of interest. For the Large Volume Flow Through Detector System (LVFTDS), which we are developing, this requirement means characterizing the basic signal produced by an alpha particle and understanding the competing signals caused by background radiation. In this report we briefly review the design of the LVFTDS, describe a series of experiments to characterize the background in the detector, explain how the data was analyzed, and report the results.

Detector Design & Background Reduction:

The key characteristic of alpha radiation that both aides and hinders its detection is the short range of alpha particles. This property aides in their detection because only a thin detector is required to stop the alpha particle and measure its energy. Other particles largely pass through such a detector depositing little energy and thus producing a small signal. The short range hinders detection in that the alpha particle will not travel far in any medium other than a vacuum. Thus for detecting alpha particles in a gaseous medium a large surface to volume ratio is required to insure that the alpha will hit a detector surface before it comes to a stop in the medium.

The LVFTDS uses a series of relatively inexpensive thin, large–area, plastic scintillator sheets to detect alphas. The thin plates minimize the sensitivity to other forms of radiation (see Fig. 1). The light created by the energy loss of an ionizing particle traversing the sheet is transmitted by total internal reflection via two lightguides to two photomultiplier tubes (PMT) which produce a charge signal that is proportional to the amount of light detected. Even with such an optimized construction the dark noise of the PMTs and the pervasive radiation background present in nature limits our ability to detect low levels of alpha emitting nuclides. In a series of experiments we have explored three techniques to improve the sensitivity of the LVFTDS.

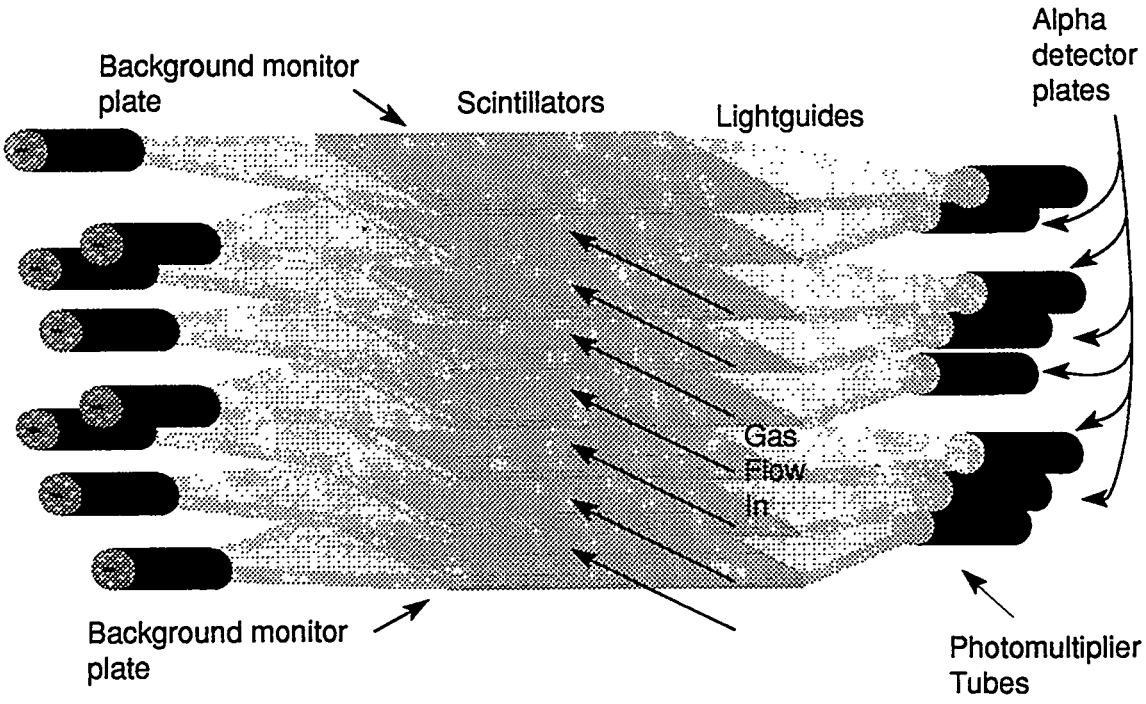

Fig. 1: Simplified schematic of LVFTDS detector showing a possible configuration with 6 alpha detecting plates and two background monitoring plates top and bottom.

Technique one simply involves placing shielding around the detector. A majority of the background radiation reaching the detector is from external sources – either naturally occurring radioactive material in the materials near the detector or cosmic rays. Even modest external shielding can significantly reduce the amount of background observed in the detector.

Technique two makes use of the short range of the alpha particle to actively discriminate against other forms of radiation. In a multi-plate detector such as we have designed, an alpha particle emitted by a nucleus will only reach and be detected by a single plate. Other forms of radiation have much longer ranges and thus will normally trigger two or more plates simultaneously (see Fig. 2). By eliminating all detected signals where two or more plates are triggered simultaneously we can discriminate against these long range forms of radiation. As an added precaution, we can surround the detector with a thick scintillator plate shield that is more sensitive to these long range forms of radiation.

The final technique involves raising the lower level discriminator of each PMT. The basic detector design has always required that for a valid signal both PMTs of a

given scintillator plate must fire above a minimum energy threshold. (The two PMT requirement is necessary because of the 2 kHz counting rate typical of a single PMT from just thermal noise.) Results presented in this report indicate that raising the minimum signal threshold in both PMTs can further reduce the background without substantially impacting the alpha detection efficiency. The remainder of this report summarizes our results in testing these various sensitivity enhancing techniques.

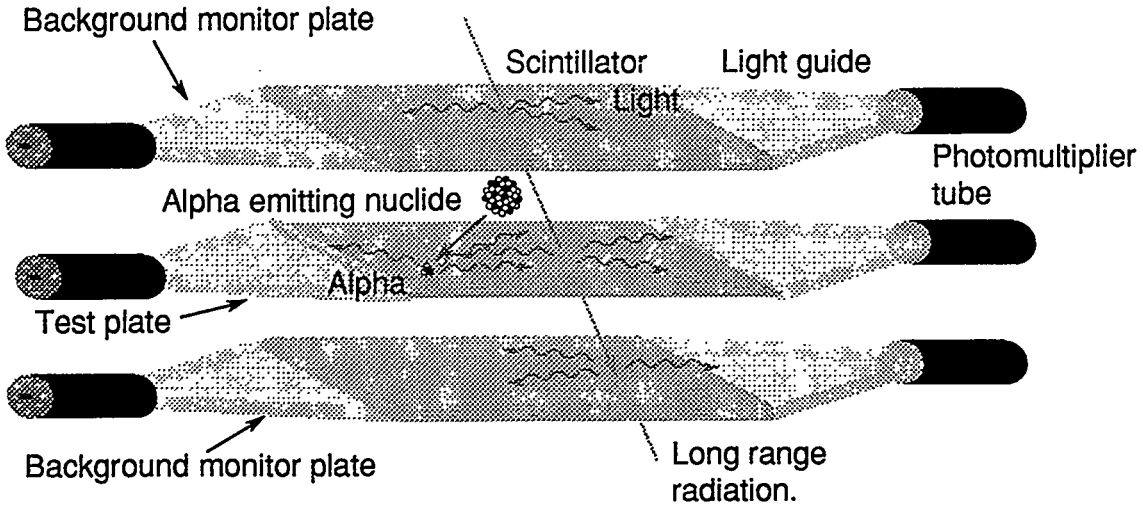

Fig. 2: Diagram indicating how alpha is only detected in single plate while most other forms of radiation will be detected in two or more plates.

Experimental Procedure

Experimental Configuration

Our basic experimental apparatus consisted of two 1 cm thick 14" by 14" scintillator plates (Bicron 400) separated by approximately 4 cm which served as background monitors (see Fig. 2). Within the gap we could place different single scintillator plates (12" by 12" Bicron 434 of varying thicknesses) which were candidate materials or geometries for the plates to be used in the final detector. Around this entire assembly we could place both a steel shield of up to 3/4" and a 2" thick lead shield (see Fig. 3). A second setup that was used for several key experiments consisted of a similar arrangement with 8 thin plates separated from each other by 2 cm sandwiched between the two thicker background monitor plates. In this latter arrangement only the top thick plate and first thin plate were used and the passive shielding was not as complete as in the 3 plate arrangement.

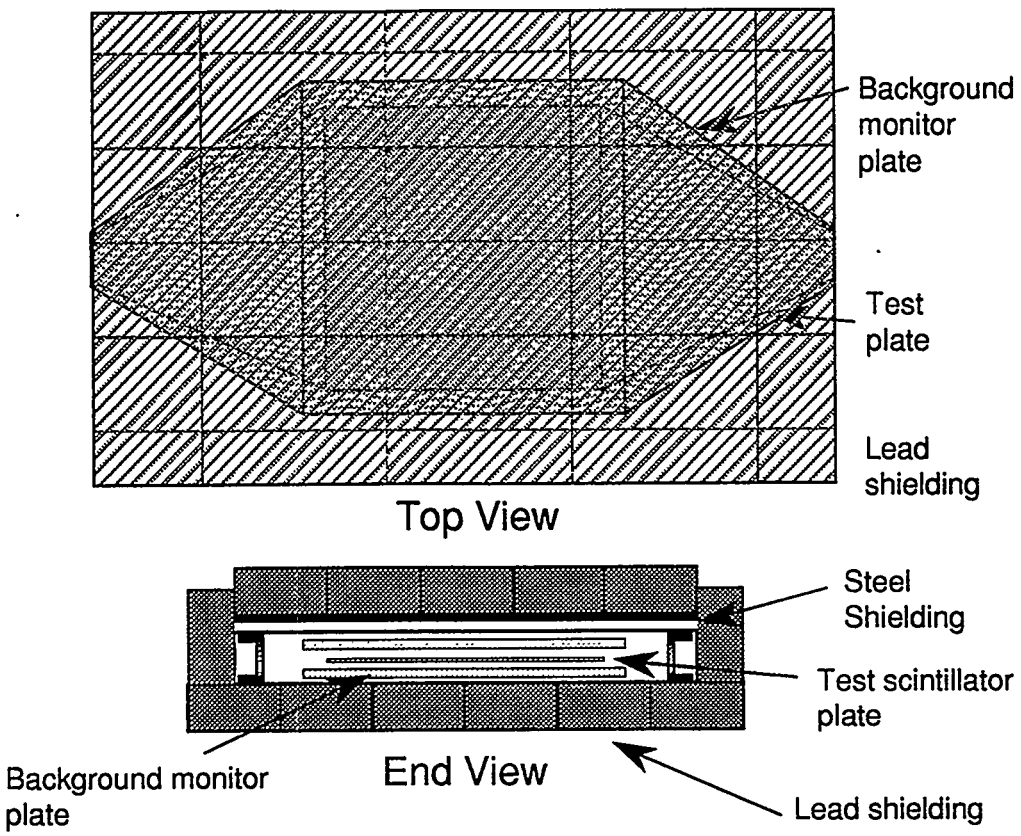

Fig. 3: Diagram of shielding setup for background reduction experiments.

Each scintillator plate consisted of the scintillator panel itself with two 3/8" thick UVT acrylic (from Polycast Corp.) lightguides glued to opposite edges of the panel. Each lightguide was connected to a PMT (Burle model 8850) via either optical grease (Dow 20-057) or RTV (Dow RTV615). Two types of lightguides were used – a symmetric lightguide and an asymmetric one. The two styles are needed to minimize the PMT mechanical interference between adjacent plates when they are optimally spaced for detection of the short range alpha particles.

Data Acquisition:

To acquire the data, the anode signal from each PMT is connected to a NIM Fast Timing Amplifier (Ortec FTA 820) followed by a NIM discriminator (EG&G CF8000). The discriminator output logic signal is converted to a 20 ns logic pulse (Phillips 758 or LeCroy 622) which is placed in coincidence (Phillips 758 or LeCroy 622) with the second PMT of the same plate. The coincidence outputs from all three plates are "OR" in a fan-in fan-out unit (LC429A) which is used to define a master trigger. Thus a single

valid event consists of one or more plates firing simultaneously. The analog signal which is fed into the CF8000 discriminator is internally split, delayed ~200 ns so that it is in time with the master trigger, and digitized using a charge sensitive ADC (LeCroy 2249w). The collected data is a list of events where each event consists of the charge signals from each of the PMT tubes when a master trigger fires. These data are transferred to an IBM PC where the list is written out to disk for later analysis.

The typical count rate of a PMT with no source present is ~2 kHz. Requiring the coincidence between the two PMTs reduces the plate count rate to ~60 Hz. With the 20 ns logic pulses (i.e. 40 ns overlap time), the chance coincidence rate is ~ 0.2 Hz or a small fraction of the background coincidence rate. As we will show this background rate of 60 Hz can be reduced by almost a factor of 50 to ~1 Hz which is still larger than the 0.2 Hz random rate. Thus the chance coincident rate is not a significant factor in determining the sensitivity of the system.

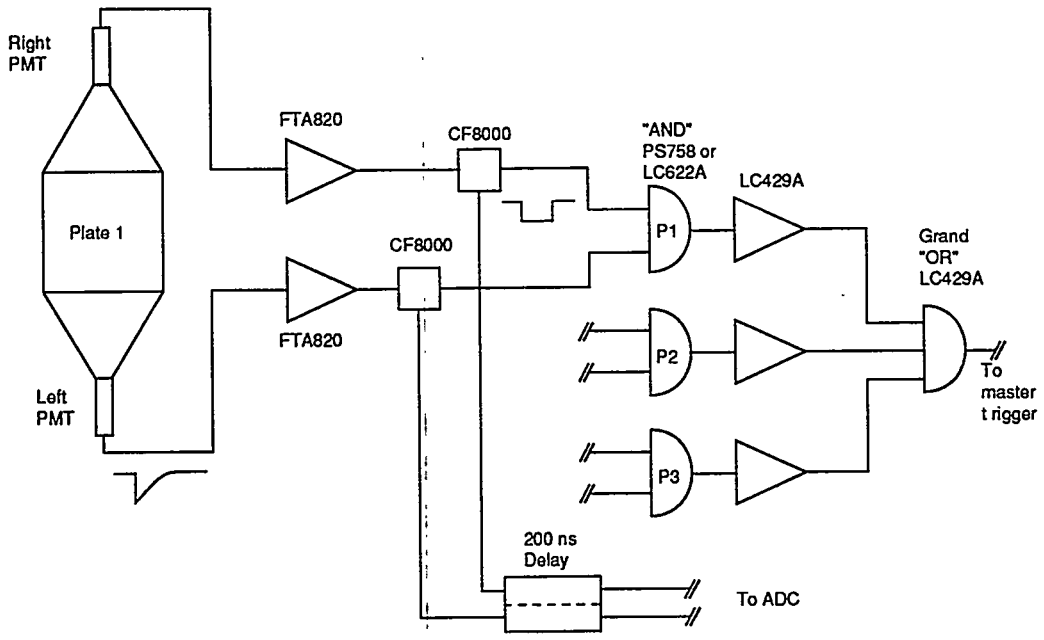

Fig. 4 Schematic of electronics system for data acquisition.

Data Analysis:

Data Description

For each configuration of the detector (e.g. with shield, without shield, with thin scintillator and symmetric lightguide, with thin scintillator and asymmetric lightguide,

etc.) we collected two types of data – a background run and a run with an alpha source present (i.e. ^{241}Am). The key information obtained during each run was a listing for each valid event (60,000 events/run) of the charge signal amplitude collected in each of the 6 PMT tubes. By analyzing the data in various ways from runs with different types of plates and/or shielding we could determine the most effective methods for minimizing the detected background radiation while maximizing the alpha particle detection efficiency.

Figure 5 shows several sample charge spectra for typical 60,000 event experiments. The key features of a spectrum include a peak at about channel 35 which corresponds to the pedestal of the ADC. A pedestal event is produced when another plate fires with no corresponding signal in the plate being histogrammed. The first broad peak corresponds to a single photoelectron being emitted by the photocathode of the PMT. The less distinct peak above the one photoelectron peak corresponds to a two photoelectron event. Higher photoelectron events are washed out by the statistical nature of photoelectron production so that one obtains a broad continuum that is roughly linear in the number of photoelectrons created and thus the amount of light collected. Because the amount of light created corresponds approximately to the energy deposited by an incident particle in the scintillator we refer to the spectra in Fig. 5 as energy spectra. The very sharp peak at channel ~2000 corresponds to all events that exceed the range of the ADC. These events are still valid and are used in the analysis, but we can only tell what their minimum energy is.

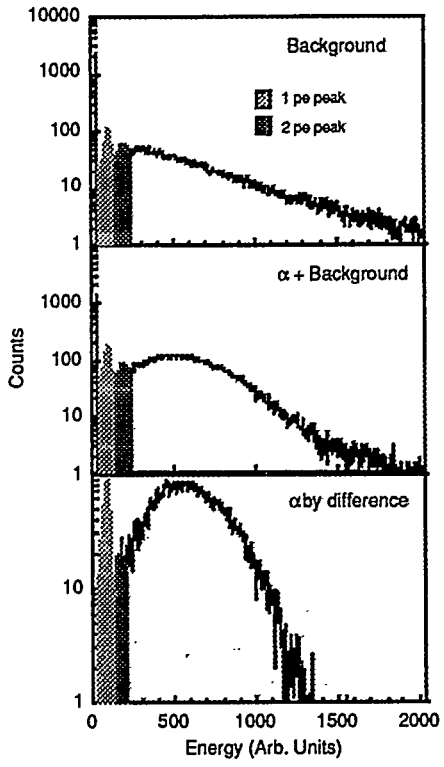

Fig. 5 Charge (energy) histogram showing background spectrum (top) with 1 and 2 photoelectron peaks identified, a spectrum with an alpha source present (middle), and the difference between the middle and top histograms which corresponds to just the alpha particles observed.

Data Analysis Procedures

Data analysis was performed by replaying the experimental event data with different gating conditions placed on each PMT signal, creating the various energy spectra, and calculating numerous integrals. A list of the gating conditions are given in table 1. As is evident from this list, we used the different gating conditions primarily to evaluate the effectiveness of various active background suppression techniques. For example, one analysis (#2) considered coincidences between the two PMTs of the test plate irrespective of signals from the other plates. Analysis (#7) considered a test plate coincidence with no corresponding signals in either background monitoring plates 1 or 2.

A substantial portion of the background causes very low energy signals in the PMTs (e.g. 1/3 is in the 1 and 2 pe peaks for the "No Shield" case of one setup), while the alphas are peaked well above the 2 pe peak. We calculated several integrals for each spectrum using different thresholds (see Fig. 5). The thresholds are: all signals greater than the ADC pedestal (1 pe +), signals above the 1 pe peak (2 pe +), and signals above the 2 pe peak (3 pe +). We also replayed the data using three different signal thresholds (i.e. above the noise, above the 1 pe peak, and above the 2 pe peak) for the coincidence requirement in both PMTs of the test scintillator plate. The goal of these tests was to preferentially eliminate the background without seriously impacting the detection efficiency of the alpha particles. The data were organized using spreadsheets in order to quantitatively compare the different analyses and runs (i.e. with an alpha source, without an alpha source, with shielding, without shielding, etc.).

Table 1: List of analyses performed on data. In cases where only two plates were used the analysis 6 and analyses 9-15 were not done. Energy thresholds for background monitor plates are always just above the ADC pedestal irrespective of alpha test plate energy threshold.

#	Description
1	No gating conditions other than hardware plate coincidence.
2	Test plate has a valid signal
3	Bkgd plate 1 has a valid signal
4	Bkgd plate 2 has a valid signal
5	Both the Test and Bkgd 1 plates have valid signals
6	Both the Test and Bkgd 2 plates have valid signals
7	Test plate is valid with no valid signal in either Bkgd 1 or 2
8	Test plate has valid signal with both PMTs above 1 pe peak & no Bkgd 1 or 2

9	Test plate has valid signal with both PMTs above 2 pe peak & no Bkgd 1 or 2
10	Test plate has a valid signal & no Bkgd 1.
11	Test plate has a valid signal with both PMTs above the 1 pe peak & no Bkgd 1
12	Test plate has a valid signal with both PMTs above the 2 pe peak & no Bkgd 1
13	Test plate has a valid signal & no Bkgd 2.
14	Test plate has a valid signal with both PMTs above the 1 pe peak & no Bkgd 2
15	Test plate has a valid signal with both PMTs above the 2 pe peak & no Bkgd 2

Results & Discussion:

Experiments:

Table 2 gives a synopsis of the primary data sets collected. In most cases both a background and a run with an alpha source were collected. The key objective of most of these experiments was to determine how much the background could be reduced without seriously impacting the alpha particle detection efficiency.

Table 2: Summary of primary experiments conducted. In most cases data sets without an alpha source (i.e. background) and data sets with an alpha source where collected for each configuration.

Series	Shielding	Notes.
P615	No Shield 3/4" steel 2" Pb + 3/4" steel	symmetric 1 mm thick plate in std. config.
P675	No Shield 3/4" steel 2" Pb + 3/4" steel	asymmetric 1 mm thick plate in std. config.
P635	No Shield 3/4" steel 2" Pb + 3/4" steel	symmetric 3 mm thick plate in std. config.
P217	No Shield 3/4" steel 2" Pb + 3/4" steel	1 mm thick asymmetric plate + 1 mm thick symmetric plate + 1 mm thick asymmetric plate.
P615 pos	3/4" steel 3/4" steel 3/4" steel 3/4" steel 3/4" steel 3/4" steel	1 mm thick symmetric plate in std. config. α source raised 6 mm off plate. α source positioned in top right corner. α source positioned in top left corner. α source positioned in bottom right corner α source positioned in bottom left corner.

P675 pos	3/4" steel	1 mm thick asymmetric plate in std. config.
	3/4" steel	α source raised 6 mm off plate.
	3/4" steel	α source positioned in top right corner.
	3/4" steel	α source positioned in top left corner.
	3/4" steel	α source positioned in bottom right corner
	3/4" steel	α source positioned in bottom left corner.
P610	No Shield	1 cm bkgd plate + 1 mm symmetric test plate
	3/4" steel	
	2" Pb + 3/4" steel	

Background Reduction - An optimized test

Table 3 gives the results for various background reduction techniques conducted using setup P615. As described above we report the background reduction results using three different thresholds set on the PMTs of the alpha detecting test plate (i.e. 1 pe +, 2 pe + and 3 pe +). The table summarizes the effects of using different energy thresholds, passive shielding configurations, active shielding conditions, and combinations of all three.

Table 3: Summary of background reduction results for 1 mm thick symmetric plate and two background monitoring plates (P615). For each shielding configuration (i.e. No Shield, S.S. Shield, and S. S. + Lead) the background is quoted as a fraction of the background present taking the full integral with no active background suppression (i.e. the entries with 1.00). Numbers in parentheses quote the cumulative background reduction when compared to the No Shield case. Error bars are approximately 5% due to normalization systematic error and statistical errors.

	Integral	Plate 1 fired	Plate 1 fired, Bkgd plates didn't	Plate 1, 2 pe + & Bkgd plates didn't fire	Plate 1, 3 pe + & Bkgd plates didn't fire
No Shield	1 pe +	1.00	0.29	–	–
	2 pe +	0.82	0.20	0.16	–
	3 pe +	0.66	0.13	0.12	0.10
S.S. Shield	1 pe +	1.00 (0.70)	0.18 (0.12)	–	–
	2 pe +	0.86 (0.60)	0.12 (0.09)	0.10 (0.07)	–
	3 pe +	0.73 (0.51)	0.09 (0.06)	0.08 (0.05)	0.06 (0.04)
S.S. + Lead	1 pe +	1.00 (0.44)	0.14 (0.06)	–	–
	2 pe +	0.86 (0.38)	0.10 (0.04)	0.07 (0.03)	–
	3 pe +	0.72 (0.32)	0.07 (0.03)	0.06 (0.03)	0.05 (0.02)

Beginning with the "No Shield" case we see that the addition of the anticoincidence condition for the active shield plates reduces the background by over a factor of 3. If we then increase the lower coincidence threshold on plate 1 to exclude the 1 pe peak, we reduce the background ~6. Finally we can also exclude the 2 pe peak which leads to an overall background reduction of ~10.

Ignoring for a moment the active background suppression, we see that by adding a steel shield and then a steel plus lead shield we obtain background reduction factors of ~1.4 and ~2.3, respectively. When we use both the active and passive shielding the factors increase to 8 and 17. If we now increase the lower thresholds to 2 pe + and 3 pe + the background reduction factors increase to 14 & 25, for the steel shield and 33 and 50 for the steel plus lead shield. These latter results indicate that the combination of passive shielding and active gating for background suppression is more effective than what one would calculate from just combining the individual shielding reduction factors. One plausible explanation for this result is that the passive shielding reduces the low–energy component of the background leaving the higher energy particles which are more likely to trigger two or more plates.

Table 4: Efficiency for detecting alpha particles using 3 plate setup for series P615. Errors are approximately 5%. Efficiencies are relative. 100% efficiency is assigned to the No Shield case with a low energy threshold just below the 1 pe peak.

	Integral	Plate 1 fired	Plate 1 fired, Bkgd plates didn't	Plate 1, 2 pe + & Bkgd plates didn't fire	Plate 1, 3 pe + & Bkgd plates didn't fire
S.S. + Lead	1 pe +	96%	97%	–	–
	2 pe +	86%	88%	85%	–
	3 pe +	81%	82%	80%	76%

A significant concern in background reduction is that the active suppression system may also reduce the efficiency of detecting alpha particles. For all the cases studied we also measured this efficiency. Table 4 gives results for the steel plus lead shield case for configuration P615. The efficiencies were calculated by taking the integrals from the alpha data, subtracting the associated background data, and dividing by the calculated normalized number of alphas expected from the source assuming that 100% were detected in the no shielding, no active background suppression case. We see that as expected the passive shielding has no effect on the efficiency of detecting alphas.

The active suppression also has no effect while raising the energy threshold of the alpha detecting plate does eliminate some of the alpha particles. This observation is not surprising when one examines Figure 5 where the difference histogram clearly shows a contribution from the 1 pe peak to the alpha signal.

Background Reduction - Supporting Results

We also tested two more realistic detector configurations compared to the optimized P615 setup. In the first configuration, P610, we set up a ten plate detector and looked at just the signals from the top background monitoring plate and the first thin alpha plate. Table 5 presents the background reduction data from this detector system in a variety of configurations while Table 6 shows the alpha detection efficiency data.

Table 5: Summary of background reduction results for 1 mm thick symmetric plate with one background monitoring plate (P610). For each shielding configuration (i.e. No Shield, S.S. Shield, and S. S. + Lead) the background is quoted as a fraction of the background present taking the full integral with no active background suppression (i.e. the entries with 1.00). Numbers in parentheses quote the cumulative background reduction when compared to the No Shield case. Error bars are approximately 5% due to normalization systematic error and statistical errors.

	Integral	Plate 10 fired	Plate 10 fired, Bkgd plate didn't	Plate 10, 2 pe + & Bkgd plate didn't fire	Plate 10, 3 pe + & Bkgd plate didn't fire
No Shield	1 pe +	1.00	0.26	–	–
	2 pe +	0.68	0.15	0.10	–
	3 pe +	0.52	0.10	0.07	0.06
S.S. Shield	1 pe +	1.00 (0.89)	0.24 (0.21)	–	–
	2 pe +	0.68 (0.61)	0.13 (0.12)	0.09 (0.08)	–
	3 pe +	0.52 (0.46)	0.08 (0.07)	0.06 (0.06)	0.05 (0.04)
S.S. + Lead	1 pe +	1.00 (0.65)	0.25 (0.16)	–	–
	2 pe +	0.69 (0.44)	0.14 (0.09)	0.10 (0.07)	–
	3 pe +	0.53 (0.34)	0.09 (0.06)	0.07 (0.05)	0.06 (0.04)

The background reduction factors using active background suppression are slightly higher for the P610 setup than for the P615 in the no shield setup even though the P615 has two background monitor plates while P610 only has one. A possible explanation for this discrepancy is that we used a more dependable technique (i.e. RTV instead of grease) to couple the PMTs to the lightguides in the P610 case than was used in

the P615 case. (We observed in the P615 case that using only one background monitoring plate instead of two increases the background by ~33%.) There exists a more significant discrepancy between how well the passive shielding works for the P615 and P610 configurations. The major difference is attributable to the construction of the P610 shielding which is not as nearly optimized as that for the P615 configuration. The less effective passive shielding produces a less effective active background suppression for P610 than for P615. This observation reinforces our earlier remark that the passive shielding appears to enhance the effectiveness of the active shielding. We believe that the passive shielding problem can be resolved for the full engineering prototype.

Table 6 quotes absolute detection efficiencies using the calibrated decay rate of the alpha source. Quoting absolute efficiencies was not possible in the P615 case because of problems with the experimental setup. However, one should note the good agreement between the relative numbers of Table 4 and the absolute numbers from Table 6 for all cases except the one that excludes the 2 pe peak.

Table 6: Absolute efficiency for detecting alpha particles using 2 plate setup P610. Note that two cases are quoted because S.S. case was done with a 65 Hz alpha source while S.S. + Lead case was done with 6.1 Hz alpha source. Error bars on S.S. case are approximately 5%. Error bars on S.S. + Lead case are larger due to the low decay rate being 15% for first column and 10% for remaining 3 columns.

	Integral	Plate 10 fired	Plate 10 fired, Back. plate didn't	Plate 10 - 2 pe + & Back. plate didn't fire	Plate 10 - 3 pe + & Anti plate didn't fire
S.S.	1 pe +	102%	102%	–	–
	2 pe +	91%	90%	84%	–
	3 pe +	74%	74%	70%	58%
S.S. + Lead	1 pe +	86%	98%	–	–
	2 pe +	70%	83%	75%	–
	3 pe +	65%	70%	64%	56%

The second configuration tested was a three plate configuration where the background monitoring plates were 1 mm thick plates (P217). This configuration is representative of the middle of the full-sized detector, see Fig. 1, where the thicker background plates will only partially measure the background in the central plates of the detector because of geometric considerations. In this case the thin alpha detecting plates

will have to measure the background for each other. Table 7 quotes the fraction of background remaining for all three shielding arrangements.

Table 7: Summary of background reduction results for 1 mm thick symmetric plate and two 1 mm background monitoring plates (P217). For each shielding configuration (i.e. No Shield, S.S. Shield, and S. S. + Lead) the background is quoted as a fraction of the background present taking the full integral with no active background suppression (i.e. the entries with 1.00). Numbers in parentheses quote the cumulative background reduction when compared to the No Shield case. Error bars are approximately 5% due to normalization systematic error and statistical errors.

	Integral	Plate 1 fired	Plate 1 fired, Bkgd plate didn't	Plate 1, 2 pe + & Bkgd plate didn't fire	Plate 1, 3 pe + & Bkgd plate didn't fire
No Shield	1 pe +	1.00	0.36	–	–
	2 pe +	0.83	0.24	0.19	–
	3 pe +	0.67	0.17	0.14	0.12
S.S. Shield	1 pe +	1.00 (0.73)	0.27 (0.20)	–	–
	2 pe +	0.86 (0.63)	0.19 (0.14)	0.15 (0.11)	–
	3 pe +	0.72 (0.53)	0.14 (0.10)	0.12 (0.09)	0.10 (0.07)
S.S. + Lead	1 pe +	1.00 (0.46)	0.23 (0.10)	–	–
	2 pe +	0.87 (0.40)	0.16 (0.07)	0.13 (0.06)	–
	3 pe +	0.73 (0.34)	0.12 (0.06)	0.10 (0.05)	0.09 (0.04)

The first observation is that the active background suppression is not as effective as when using the thicker background monitoring plates (compare Table 7 to Table 3). Our calculations indicate that a 1 cm thick plate is required to measure close to 100% of the background beta and muon radiation incident on the plate. However, the background suppression efficiency using the 1 mm plates is surprisingly good. The thicker plates are only 1.5 - 2.0 times more effective. Because the detector is constructed of many thin plates with each one capable of acting as a background detector for the remaining plates we believe that active background suppression should be almost as effective in the center of the detector as near the thicker background monitoring plates. This idea is now being tested in the full-scale scientific prototype.

Background Reduction - Other Tests

3 mm thick detector

With setup P635 we explored using a thicker plate, 3 mm opposed to 1 mm, as the basic detector element for the LVFTDS with the idea that such a plate would have a higher efficiency for detecting the background radiation and thus better optimized for the active background suppression technique. With the P635 setup we were able to determine whether the active background suppression system using 1 cm thick plates could reduce the background to the same level as in the P615 setup. For almost all cases the background still remaining in the 3 mm plate was 2.0 times higher than in the 1 mm plate. Indeed the active background suppression factors were consistently lower for this setup than the P615 setup indicating that background events detected by the 3 mm plate were not being observed with 100% efficiency in the thick background detection plates.

A comparison was made between P635 setup which approximates a detector with 3 mm plates through out and the P217 setup which models a detector with 1 mm plates. (This comparison is not strictly valid because the comparison is weighted in favor of the P635 case which has the two 1 cm background monitoring plates.) In all cases the background in the P635 system was 1.5-2.0 times higher than for the P217 setup. So even with a configuration optimized for background detection, the 3 mm plate consistently had higher backgrounds than the 1 mm plate. This test validates our original idea that for alpha detection the plates should be as thin as possible to eliminate background from the outset.

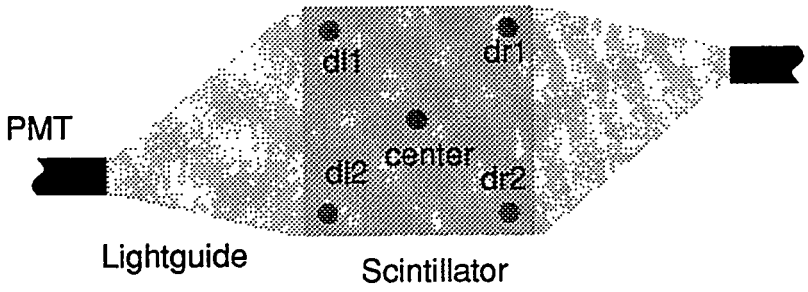

Fig. 6. Schematic of plate with asymmetric lightguides. Dots represent positions where efficiency tests with an alpha source where conducted.

α detection efficiency

We conducted tests to check the alpha detection efficiency as a function of position by placing an alpha source at each of the 5 positions indicated in Fig. 6 for both

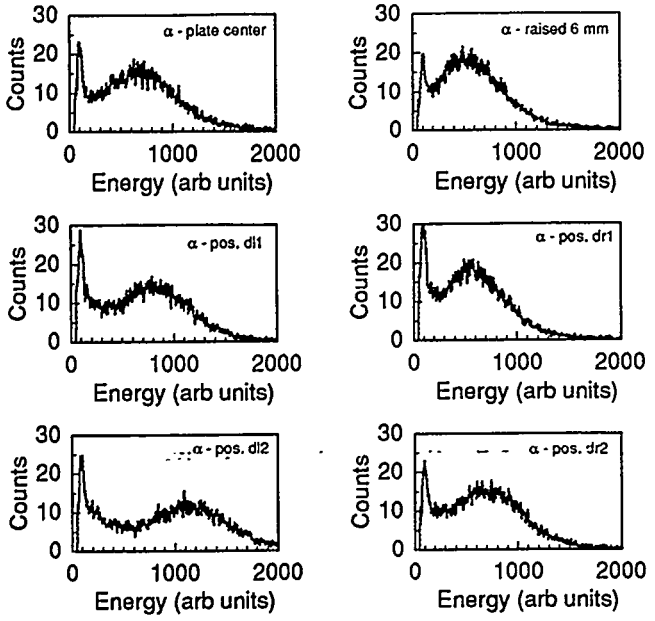

Fig. 7. Spectra of position tests with alpha source in different positions on scintillator connected to asymmetric lightguides..

the symmetric and asymmetric lightguides. Fig. 7 shows the resulting alpha spectra obtained in the PMT (i.e. the left PMT in Fig. 6) for each position with the requirement that both PMTs fired above the noise for a valid event (only results for asymmetric case are shown). Position dl2 has the highest energy peak which is not surprising considering that position dl2 is located nearest the PMT. Spectra for positions dl1 and the center are about the same and have a peak that is lower in energy than dl2 while the spectra for dr1 and dr2 have even lower energy signals. The alpha source was also placed at the center position, but raised 6 mm off the scintillator plate so that part of its energy was lost in air (i.e. energy loss ~10%). The energy peak is downward shifted from the center position case.

Table 8. Alpha detection efficiency for alpha source at various positions on scintillator connected to asymmetric lightguides. All results are normalized to the center position case, 1 pe + integral. Errors are approximately 5%

	1 pe +	2 pe +	3 pe +
Center Pos.	100%	90%	85%
Pos. dl1	101%	88%	83%
Pos. dl2	101%	88%	79%
Pos. dr1	106%	93%	86%
Pos. dr2	97%	87%	81%
Center pos. raised 6 mm	94%	87%	80%

Quantitative results are given in table 8 where we record the alpha detection efficiency for the 1 pe +, 2 pe + and 3 pe + cases with only a coincidence requirement in the asymmetric plate. (All results were normalized to 100% efficiency for plate

coincident case with no anticoincidence requirement. The results are very similar to those reported in table 4 indicating that within the errors the detection efficiency is independent of alpha incident position and lightguide design. This result is supported by Fig. 7 where the energy peak due to the alpha is always well separated from and above the 1 pe peak.

Sensitivity:

The key finding from our experiments is that by using a combination of both active and passive background reduction techniques the background can be reduced by a factor of ~10 (results from p217 case). Additionally, if we use an energy threshold in each PMT that is just above the 1 pe peak we can further reduce the background by another factor of ~2.0 with only a ~10% reduction in alpha detection efficiency. From this result we can calculate the detection sensitivity for a given plate by using the measured background counting rate.

For configuration P610 we have a plate 1 background count rate of ~350 counts/min. using a single 1 cm thick plate for active background reduction, a 2" thick lead shield, and an energy threshold just above the 1 pe peak in the 1 mm thick alpha detection plate. With the background characterized by the detector itself in a 1 minute count we can calculate the number of alpha particles that need to be detected within 1 minute to obtain a two sigma signal:

$$\text{Count}_{\text{min}} \approx 2 * \sqrt{2 * \text{count} / \text{rate}_{\text{min}}}$$

which in our case gives 53 counts/min. For our 1 plate counter with an active volume of ~1.9 liters the measured background rate translates to a sensitivity of 14 picoCuries/liter. Extrapolating this number to that of the proposed engineering prototype, which has an active volume of ~20 liters, the sensitivity becomes ~4 picoCuries/liter. In practice this number can be reduced to less than 3 picoCuries/liter because the background can be characterized over a longer period of time thereby changing the factor of 2 under the square root sign to ~1.

Figure 8 shows how dramatic the use of active and passive background reduction with a 2 pe + energy threshold is in picking out the alpha signal from the background. The top left figure shows the background, a low level alpha source and background, and the alpha signal derived from taking a difference of the first two spectra when no background reduction techniques are employed. The bottom left figure shows the same data, but now taken with a 2" lead and 3/4" steel shield. The top right figure is with active background suppression on and a 2 pe + energy threshold. The bottom right figure combines passive

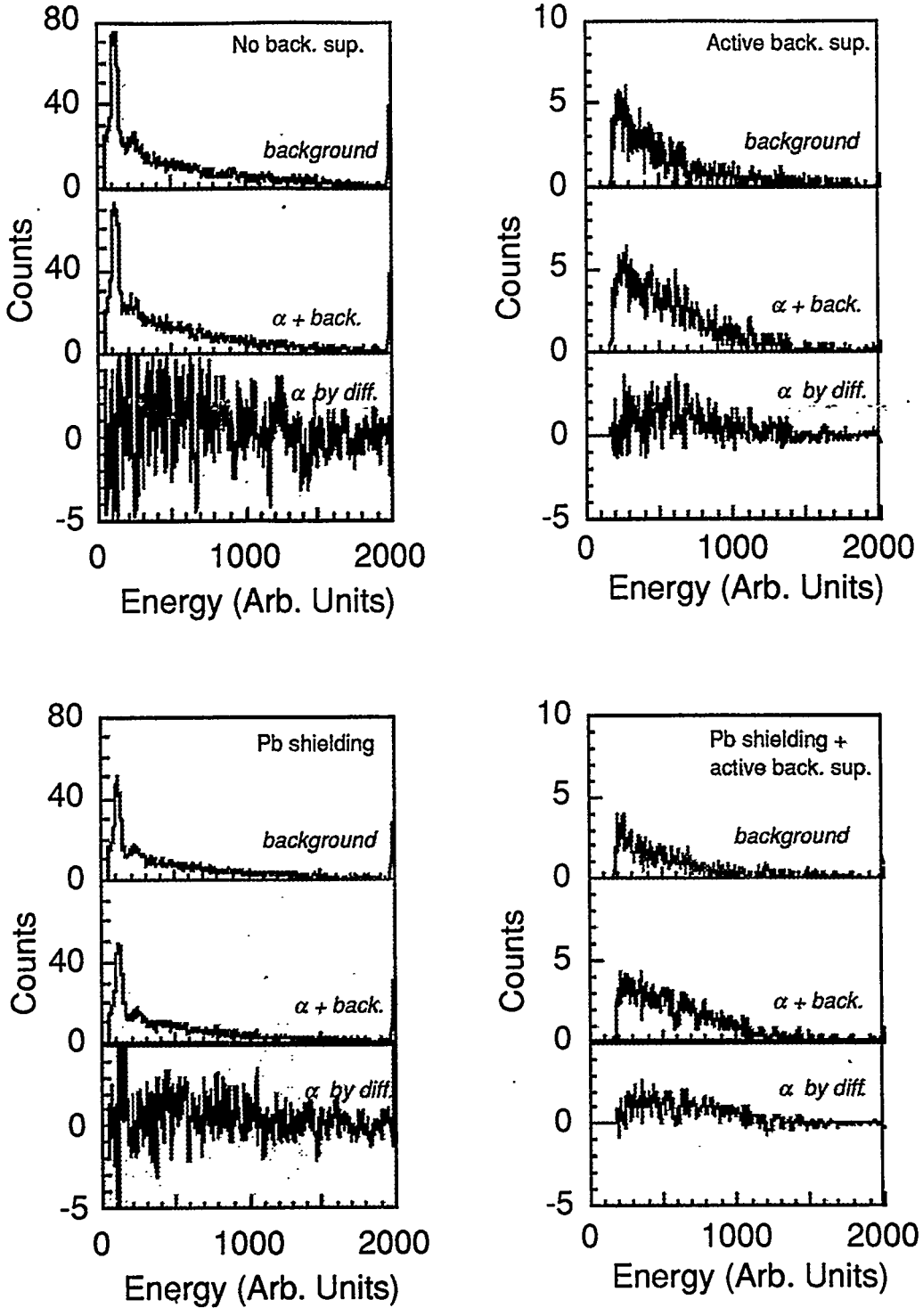

Fig. 8: Spectra showing effectiveness of background reduction techniques. In each figure the spectra are background, alpha plus background, and alpha by difference using the first two spectra. Note change in Y scaling between left and right sets of figures.

and active background suppression along with the energy threshold. In the last set of spectra the alpha signal is clearly visible while in the first set of spectra the alpha signal is not discernible.

Conclusion:

We have described an extensive set of experiments aimed at increasing the sensitivity of the LVFTDS by a combination of background reduction techniques. Our results indicate that by using a combination of passive shielding, active background suppression, and a modest energy threshold the background can be reduced by over a factor of 20. Such a decrease in background should lead to an alpha detection sensitivity a factor of 5 higher than without using such techniques. A conservative estimate based on results from these experiments indicates that a 20 liter detector should have a sensitivity of better than 3 picoCuries/liter in a 1 minute count. Experiments using a scientific prototype detector with 10 plates and a 20 liter active volume are now in progress to verify that with use of the background reduction techniques discussed in this report the LVFTDS can reach the predicted sensitivity.

LA-UR-94-2930

Title: Development of a Once Through Flow Test Apparatus for a Real-Time Monitor for Airborne Alpha Emissions

Author(s): Christopher J. Darr

Submitted to: Summary report of summer student project

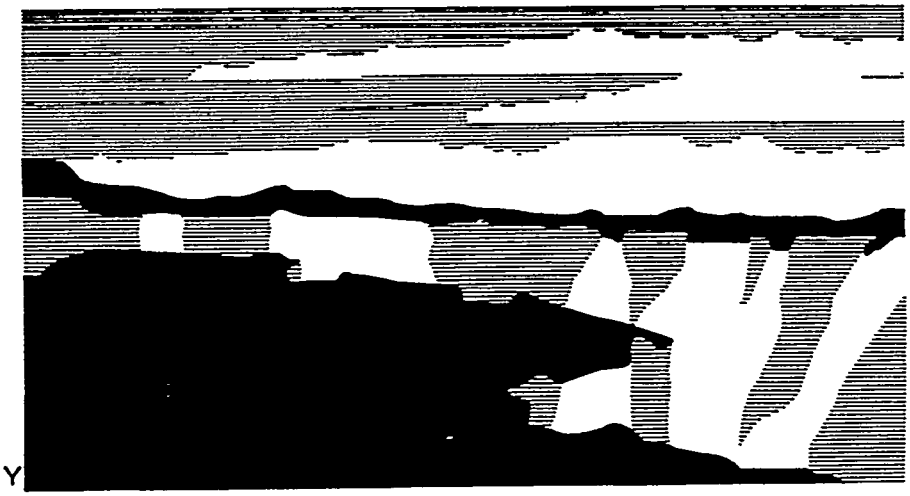

Los Alamos
NATIONAL LABORATORY

Form No. 836 R5
ST 2629 10/91

Appendix B

Development of a Once Through Flow Test Apparatus for A Real-Time Monitor for Airborne Alpha Emissions

Los Alamos National Laboratory

Development of a Once Through Flow Test Apparatus for a Real-Time Monitor for Airborne Alpha Emissions

Christopher J. Darr

Background

The growing concern for the environment has led to more careful monitoring of materials that are exhausted into the atmosphere. Radioactive waste, a major concern, has some of the most stringent handling and disposal safety rules. The United States has constructed several waste incinerators to effectively reduce the volume of the waste. The incineration process produces an off-gas which potentially contains low levels of alpha emitting nuclides. This problem requires an adequate way to detect the radioactive nuclides and shutdown the incinerator to minimize the emission of radioactive material into the atmosphere.

Several continuous air monitors that can detect low level radiation are commercially available. The disadvantage to these detectors is that they only sample a small portion (1 - 2 cfm) of the air that passes through the stack. These detectors also incorporate some kind of particulate filter, resulting in a progressive buildup of particles which can decrease the monitor's sensitivity. To effectively monitor the stack gas, the detector must sample a large detection volume, have a short integration or response time, and constant sensitivity.

A new method of monitoring the exhaust air is examined in the Large Volume Flow Through Detector System (LVFTDS). Unlike traditional filter systems as described above, the LVFTDS measures radiation levels by use of an array of thin scintillator plates. There would be no particle buildup with this method and the entire volume of air can be ducted into the detector without disrupting the airflow (the detecting volume in the current configuration is 17.5 liters (4.6 gallons)). This large detection volume enables the entire stack gas or room exhaust to pass through and be monitored with high sensitivity and short integration times.

Introduction

Through other experiments concentrating on the effectiveness and efficiency of the scintillator plates and photo multiplier tubes to see low level radiation, the concept of detecting alpha activity has been proven. The first generation prototype, which re-circulated ^{220}Radon gas around a five scintillator plate stack demonstrated that the scintillator would be able to detect the presence of radioactive gas over natural background events. The Once Through Flow test is a second generation prototype that brings the LVFTDS closer to field application. This experiment will consist of moving an air/Radon gas mixture through the detector to determine the efficiency of detecting low radiation levels in a constant air exchange. The once through flow test will use ten scintillating plates, two 1cm thick (14" square) anti-coincidence plates, and eight 1mm thick (12" square) plates that will comprise the sensitive detector area.
To conduct this test, it is necessary to modify the detector box to accommodate the 10 plate stack, adequately duct the airflow into and out of the box, properly shield the box (use of Lead and stainless steel), while ensuring light tightness.

Preliminary Tests

Fume hood Ducting

To eliminate the hazard of Radon gas leaking out of the confines of the flow guides within the detector and outlet hose. it was proposed that the laboratory fume hood would be used to pull the air through the detector. The fume hood was blocked off and an opening for a 4" diameter hole was made. By using an Omega Air Velocity Meter (HHF6002) the air velocity of the 4" hole was measured using the Log-linear traverse for round ducts. two diameter approach[1].

The governing equation for determining air velocity is:

$$Q = V_a * A \qquad \text{Equation 1.}$$

Q = flow rate

V_a = average velocity

A = area of a circle (πr^2)

The average velocity for the 4" hole, V_a = 1184 fpm

$A = 0.0873\ ft^2$

$Q = V_a * A = 1184\ fpm * 0.0873\ ft^2 = 103.3\ cfm$

This flow rate seemed too low to provide adequate air exchange so the hole diameter was increased to 6" diameter. Using equation 1,

$A = 0.1963\ ft^2$

V_a = 1220 fpm (as measured using Log-linear method)

$Q = V_a * A = 1220\ fpm * 0.1963\ ft^2 = 239.5\ cfm$

This airflow twill provide an air exchange in the detector comparable to the recirculating tests done earlier.

After selecting the air velocity, the air exchange rate through the sensitive volume was estimated:

Stack Height = 8.2 in

Scintillator Plate Area = 12 in * 12 in = $144\ in^2$

Sensitive Volume = 8.2 in * $144\ in^2 = 1180.8\ in^3 = 0.683\ ft^3$

$$\text{Time for Total air Exchange} = \frac{\text{Volume}}{\text{Flow rate}}$$

$$\text{Air Exchange} = \frac{0.683\ ft^3}{336\ cfm} = 0.02033\ \text{min.} = 0.122\ \text{seconds}$$

This calculation shows there will be a theoretical total air exchange every 122 milliseconds.

An acceptable diameter was chosen for the airflow so that it was possible to purchase the same diameter PVC piping to construct the inlet and outlet ports for the

detector. It was necessary to determine the number of bends necessary to eliminate any light from entering the detector that would interfere with the radiation measurements and possibly damage the photo multiplier tubes.

Several lengths of flat black flexible exhaust tubing were used to find the minimum number of bends. This was a simple test consisting of placing a flashlight in one end of the tube and bending it until the light could no longer be seen. The result of this test was the tube needed at least three 90° bends. Several PVC elbows and tank adapters were purchased to attach the tubing to the detector and the fume hood. To reduce light each piece of PVC was painted flat black. The flexible tubing was then attached to the inlet and outlet and also attached to the fume hood (Figure 1.)

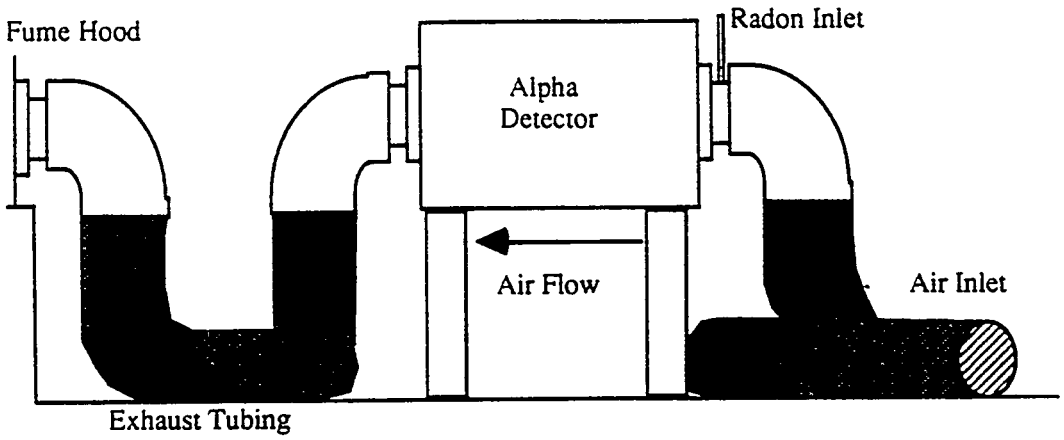

Figure 1. Schematic of arrangement of air ducts for tests.

This exhaust tubing is 8" in diameter so hose clamps and 2" wide black electrical tape was used to ensure a good seal to the PVC elbows. Each exhaust tube is 9.25 ft (2.82m) long. The inlet has two hoses (18.5 ft) taped together for light tightness and is coiled under the detector box; outlet length is 9.25 ft.

Darkness Test

To ensure that the box with inlet/outlet ports was still light tight, a series of experiments were conducted to test the darkness.

Tube used for experiment: Chekov (Burle 8850)

1 photo-electron (pe) peak: Channel 91

Full Width Half Max. for 1pe peak: 54%

Voltage: 2080

To gauge the amount of light that may be entering the box, a singles rate was taken each time. A singles rate is the number of events registered over a certain amount of time (in

this case, 10 seconds). The PMT end window was covered with black electrical tape to get a singles rate of the "dark" current (absolutely no light).

Rate: 1156.9 Hz

The tape was removed and the PMT placed facing into the outlet port.
The measured rate of 16500 Hz indicated considerable light leaking into the box. To determine where the light was entering, the exhaust hose was disconnected and the PVC elbow capped. The rate was unchanged, it was hypothesized that perhaps photons were still going through the blackened PVC. The elbow was therefore wrapped in black plastic and rates taken again.

Rate: ≅ 350 Hz

This proved to be a much more satisfying rate. It was found that the combination of flat black paint and black plastic would be effective in providing good light tightness.
The PMT was placed in the inlet hole and a similar test was done. The PVC was wrapped in black plastic as well.

Rate: 495 Hz

This test was adequate to prove that the box is indeed light tight and that preparation for the 10 plate stack could continue. The inlet and outlet rates are substantially lower than the dark current rate (which theoretically should be the lowest rate). The reason for this is the tube had not gone under a full dark conditioning. If another dark rate was taken after the inlet test, it would be lower than the inlet/outlet rates.

Alpha Detector Design

Box Modifications

The box that was used for the Radon recirculation[2] experiment was also being used for the Once Through test. This required that the flow guides be modified and new parts be constructed. The re-circulatory test contained side flow guides, a top and bottom plate, and two muffin fans to move the air/gas mixture (Figure 2.)

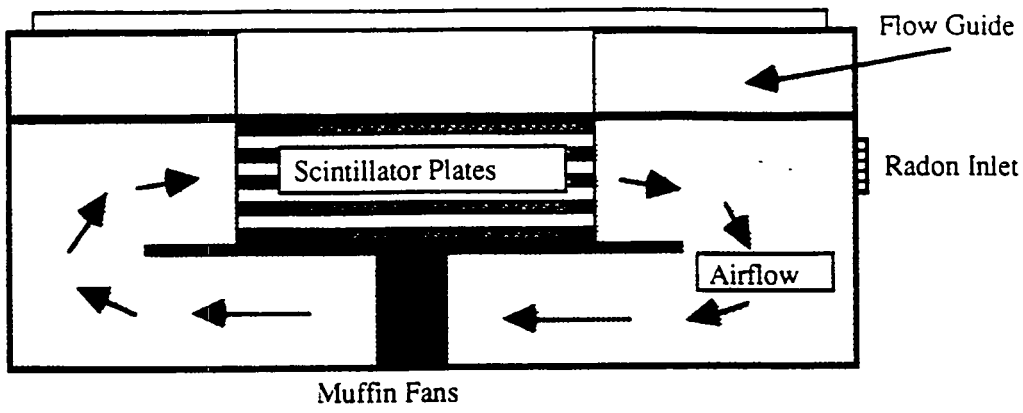

Figure 2. Re-circulatory Experiment Setup

The Once Through test required that more space be allocated for the scintillator plates, only 5 plates were used for earlier test, whereas this test would be using a 10 plate stack. This configuration would also require complete lead shielding on all sides of the detector. To accomplish this, the flow guides needed to be modified to accommodate the steel frame that would support the stainless steel and lead bricks that would cover the scintillator plates. The modification also required that the flow guides be widened to accommodate the two 14" anti-coincidence scintillator plates.

The box used for the first prototype is a NEMA type-4 enclosure 91 cm X 152 cm X 52 cm (36 in X 60 in X 21 in). This commercially available steel enclosure has a gasket hinged lid. This box proved to be both air and light tight in the re-circulatory test and therefore has also been used for the Once through test. Two 7.25in. diameter holes were cut into the 152 cm sides of the box to hold the 6in. tank adapters to attach the PVC joints and elbows.

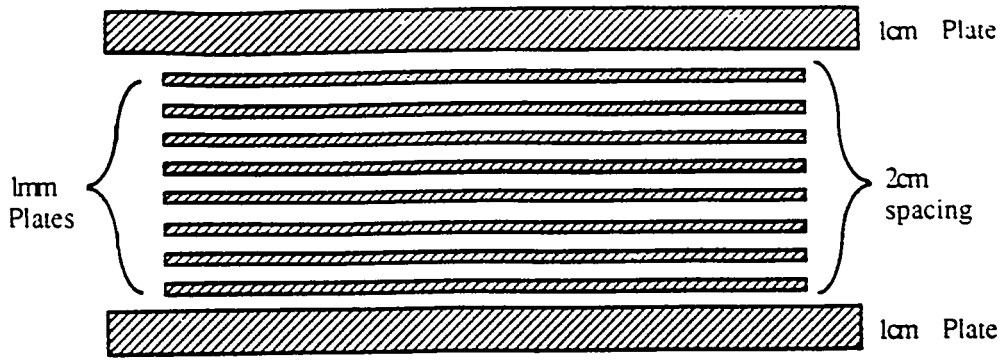

Figure 3. Scintillator Stack

The 0.25in plexiglass flow guides in the first experiment spanned the entire height and length of the box (91 cm X 52 cm). These needed to be cut down to allow for stacking of the lead brick shield that would be placed above it. The former test used five 12in square scintillator plates(Figure 4a.), while this test would have two 14in square plates and eight 12in plates stacked 2cm apart within the 14in plates. (Figure 3.) there needed to be a way to install and seal the 14in plates, and install the 12in plates and have them sealed as well. This was accomplished by widening the flow guides to 14+in (to allow for closed pore weather stripping) and placing spacers between the top and bottom

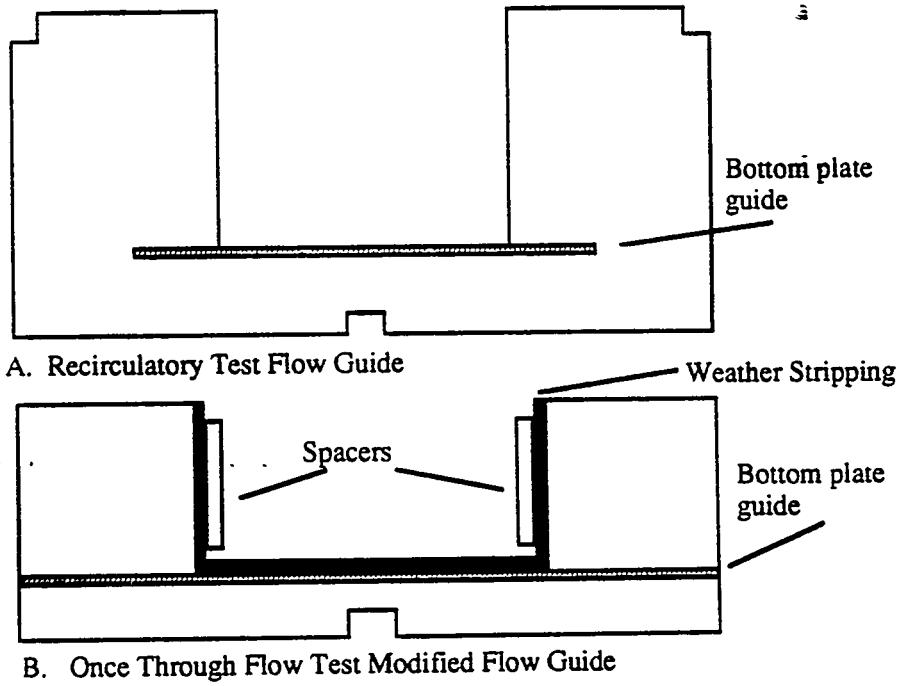

Figure 4. Flow Guide Modification

anti-coincidence plates (Figure 4b.). In the analysis of the previous three plate stack

tests[3], it was found that the best background reduction in passive shielding was the use of 304 stainless steel (0.75in) and lead bricks (2in). The area under the scintillator and light guides was lined with 2in X 4in x 8in lead bricks. Lead was also placed on the sides of the flow guides. The stainless steel essentially serves two functions, to shield the scintillator and support the lead bricks. The frame is constructed from cold rolled C2X2.25 steel and TIG welded and is large enough to cover the scintillator and the light guides.

Notice in figure 4. there is a square portion subtracted from the bottom of the flow guide. The steel enclosure has a 1/2in square brace along the length of the floor. This could not be removed as it would weaken the box's structural integrity. To overcome this small barrier, six pieces of 1/2in plywood were laid in the bottom of the box (Figure 5.) to essentially raise the floor. The flow guides allow for this brace and are attached (using RTV) directly to the steel interior. The plywood provided an even surface for the lead to be laid on.

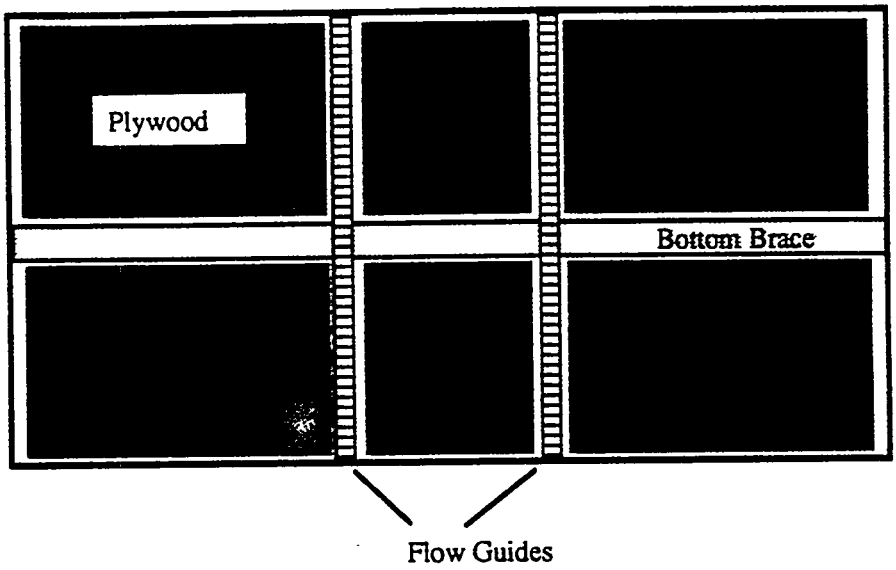

Figure 5. Top View of Enclosure

Data Acquisition

The data collection system consists of NIM and CAMAC modules controlled by an acquisition code programmed in Quick BASIC by Russell Gritzo and Malcolm Fowler. This code, named ADCSPECH.BAS (ADC SPECtrum version H.) is used to read the CAMAC, plot the ADC spectra, and save the data to disk for further analysis.

When an alpha particle, beta or gamma ray hits the Bicron scintillator plate, photons are produced and they travel through the plate to the UVT light guides and into the Burle 8850 photo multiplier tube (PMT). The photons hits the photo cathode, are converted to an electrons which bounces around the dynodes in the PMT, creating a cascade proportional to the energy deposited in the scintillator by the original particle. This cascade is converted into an analog electrical signal by the PMT base (Canberra Model 2107) and enters the data acquisition system (Figure 6.) through the Fast Timing Amplifier (Ortec FTA820).

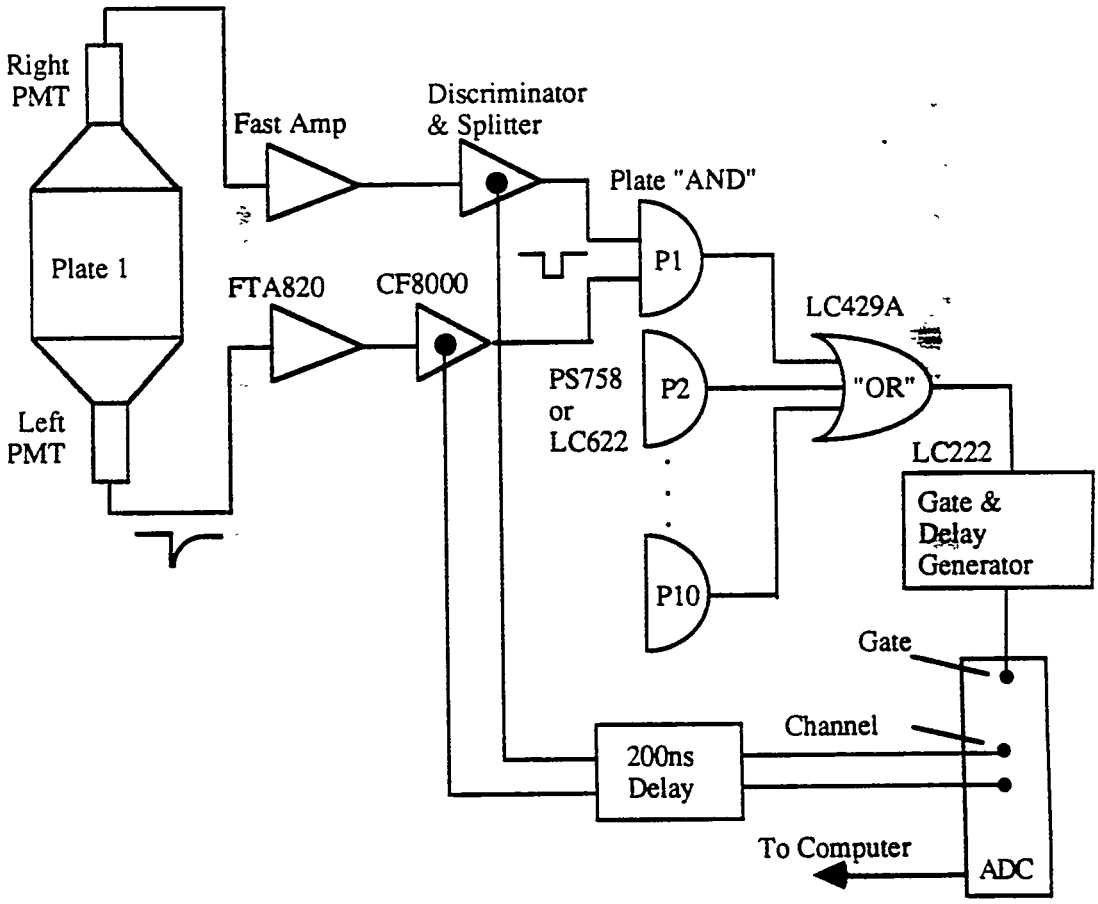

Figure 6. Data Acquisition Logic Diagram

The analog signal is then split by the Octal Constant Fraction Discriminator (EG&G CF8000) and sent to a 200 nano-second delay. The output from the CF8000

discriminator is sent to a Logic Unit (Phillips Sci. 758) or Quad Coincidence (LeCroy 622). A plate "AND" is generated when both PMTs see the same event. Each scintillator plate undergoes this same treatment and is then placed into a grand plate "OR". The grand "OR" goes to a Dual Gate Generator (LeCroy 222) and creates the gate for the ADC. The signal that was delayed 200ns from the discriminator is then received by the ADC and recorded by the data acquisition code ADCSPECH.BAS. This code interprets the data and creates a spectra plot.

Appendix A Detector Box Drawings

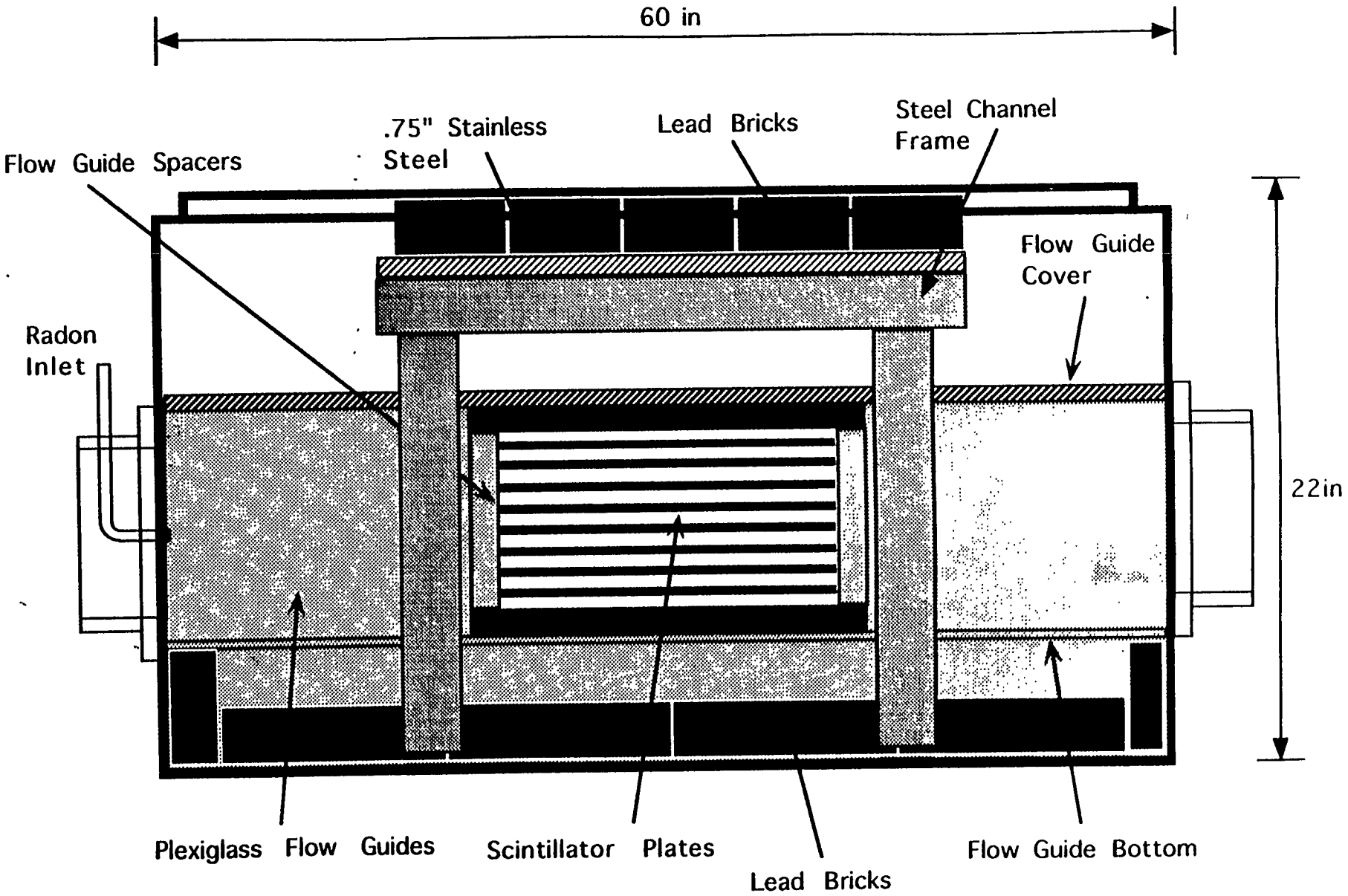

Drawing 1. **Alpha Box Interior Assembly** End View

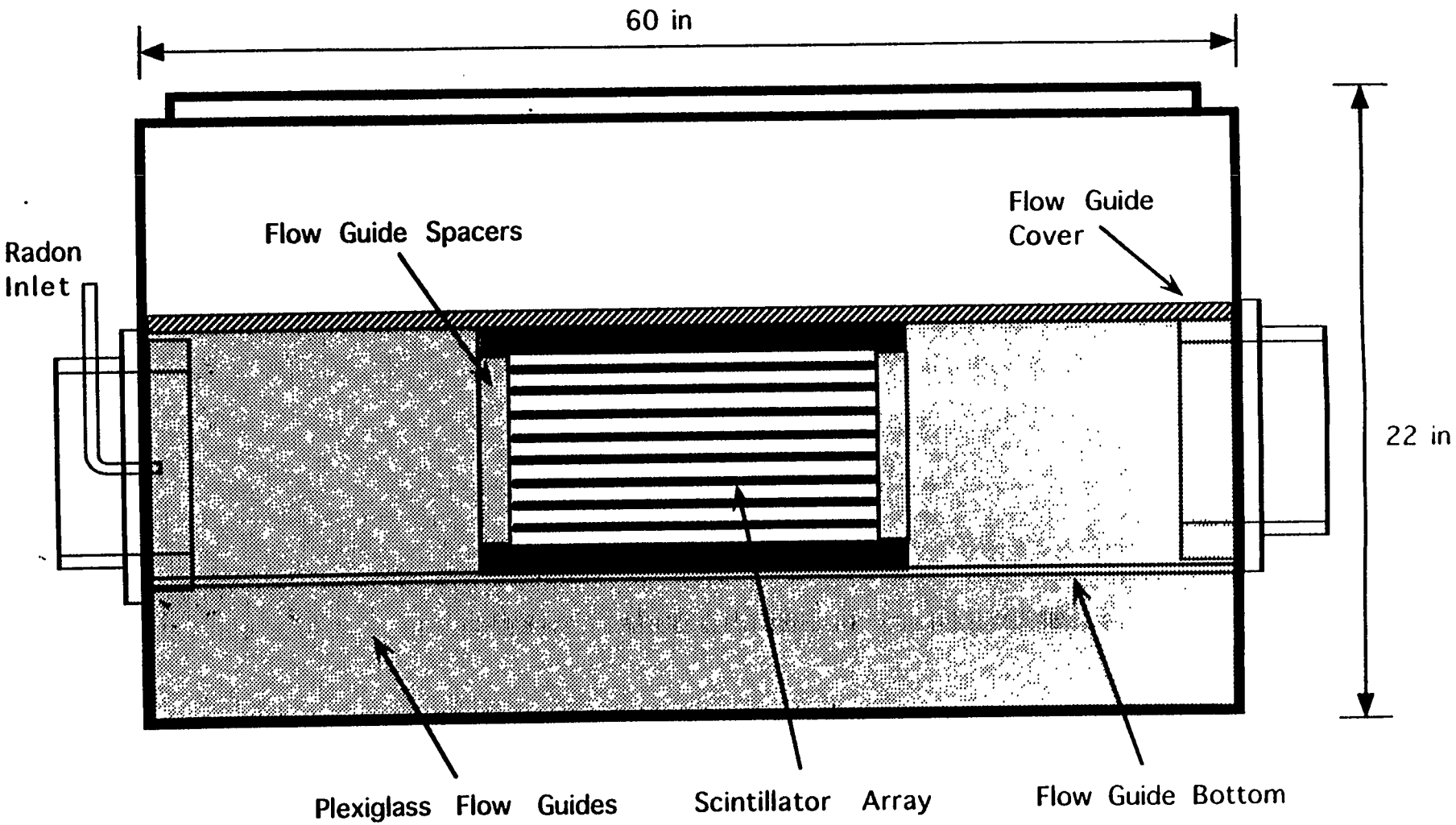

Drawing 2. **Alpha Box Showing Flowguides** End View

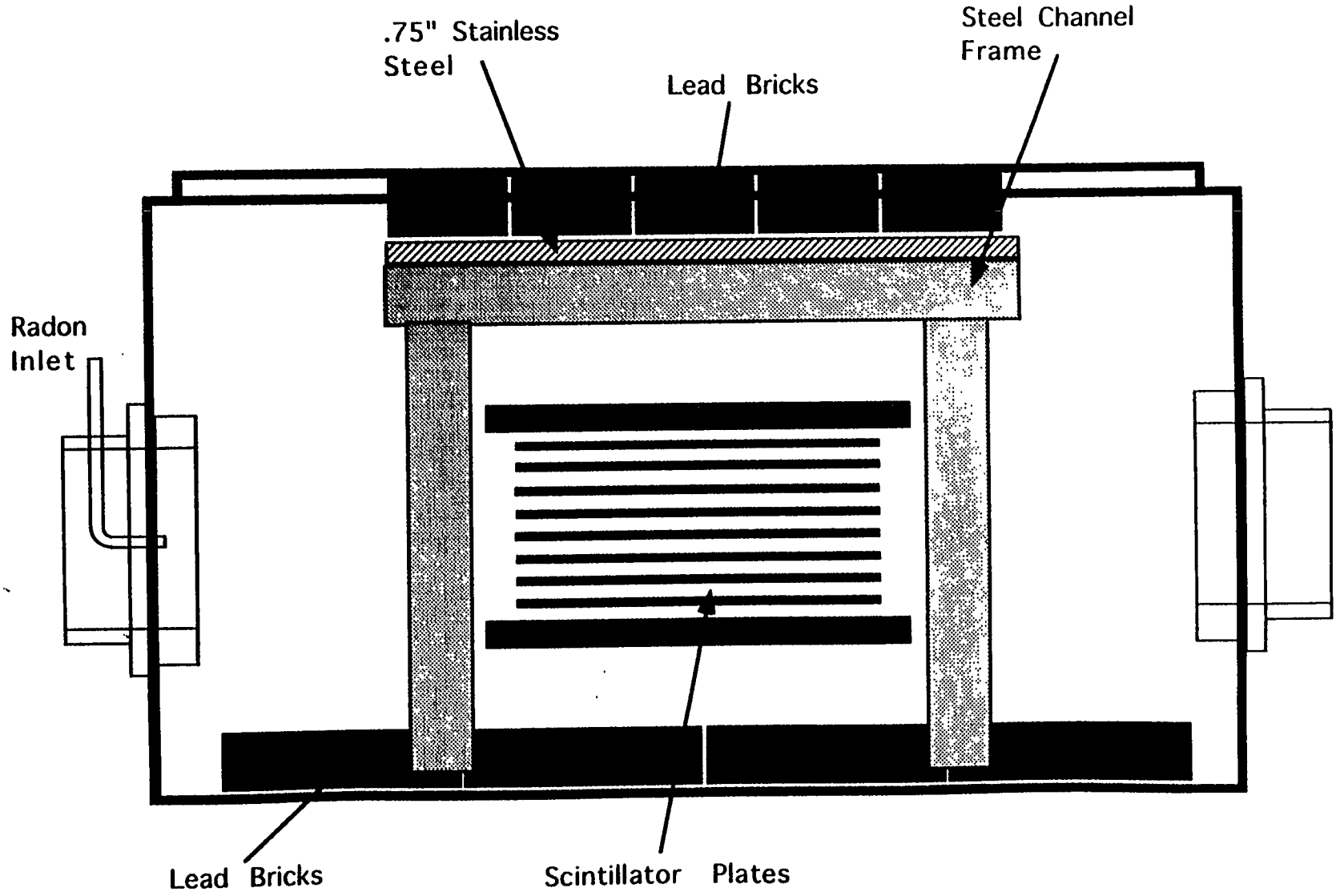

Drawing 3. **Alpha Box Showing Stainless Steel Frame Assembly** End View

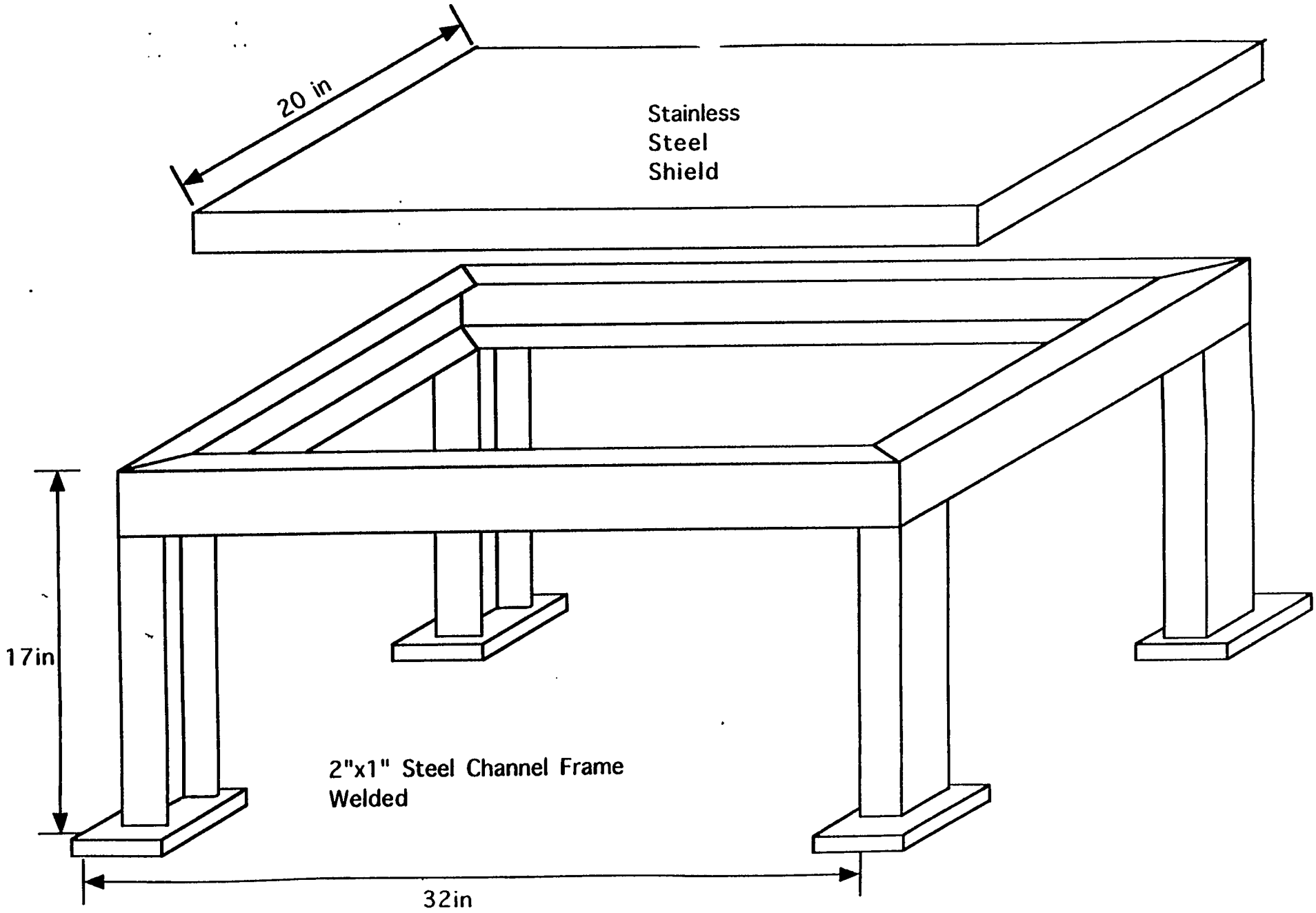

Drawing 4. Steel Frame Support for Stainless Steel & Lead Shield

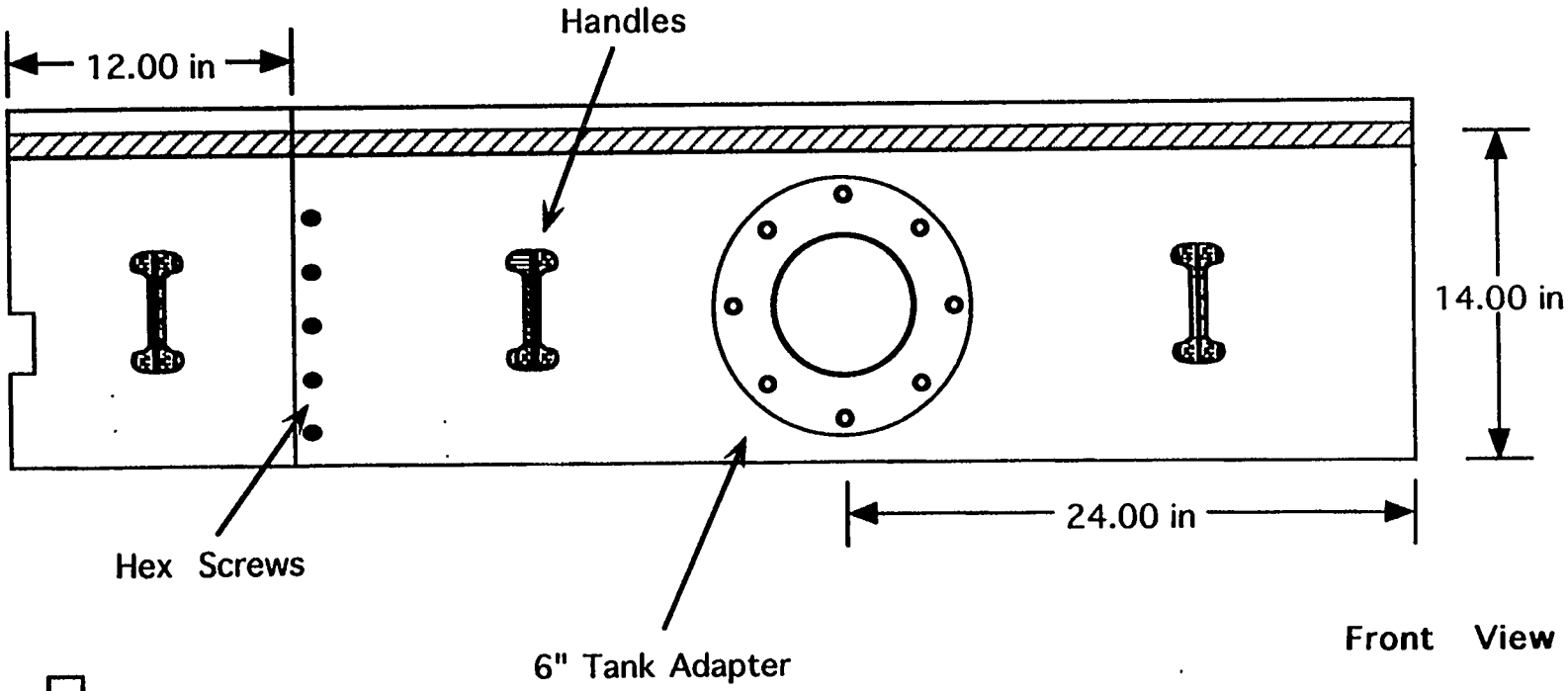

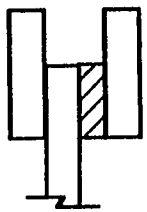

Side View

Drawing 5. **Fume Hood/ LVFTDS Airflow Connection**

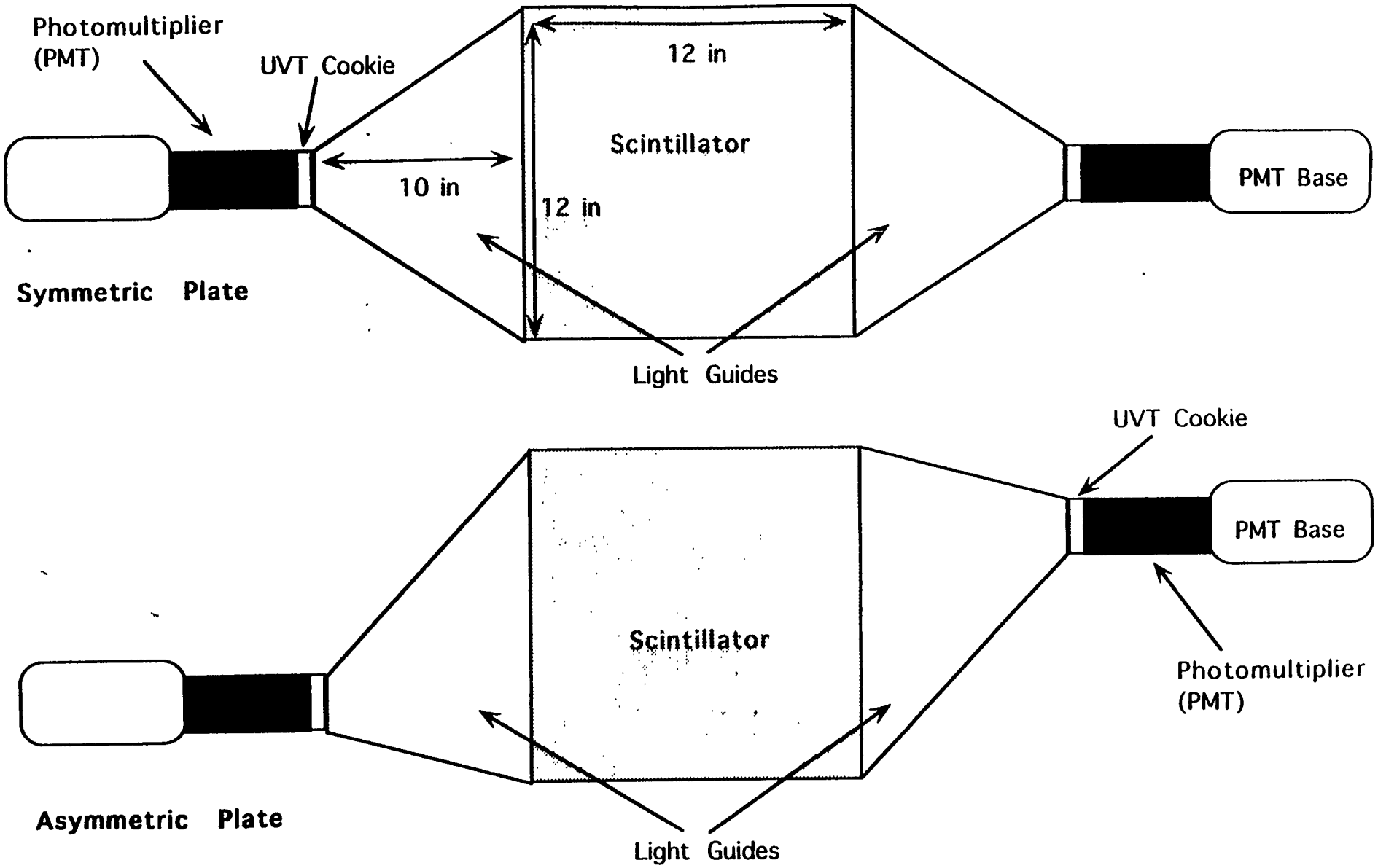

Drawing 6.

Scintillator Plates

Top View

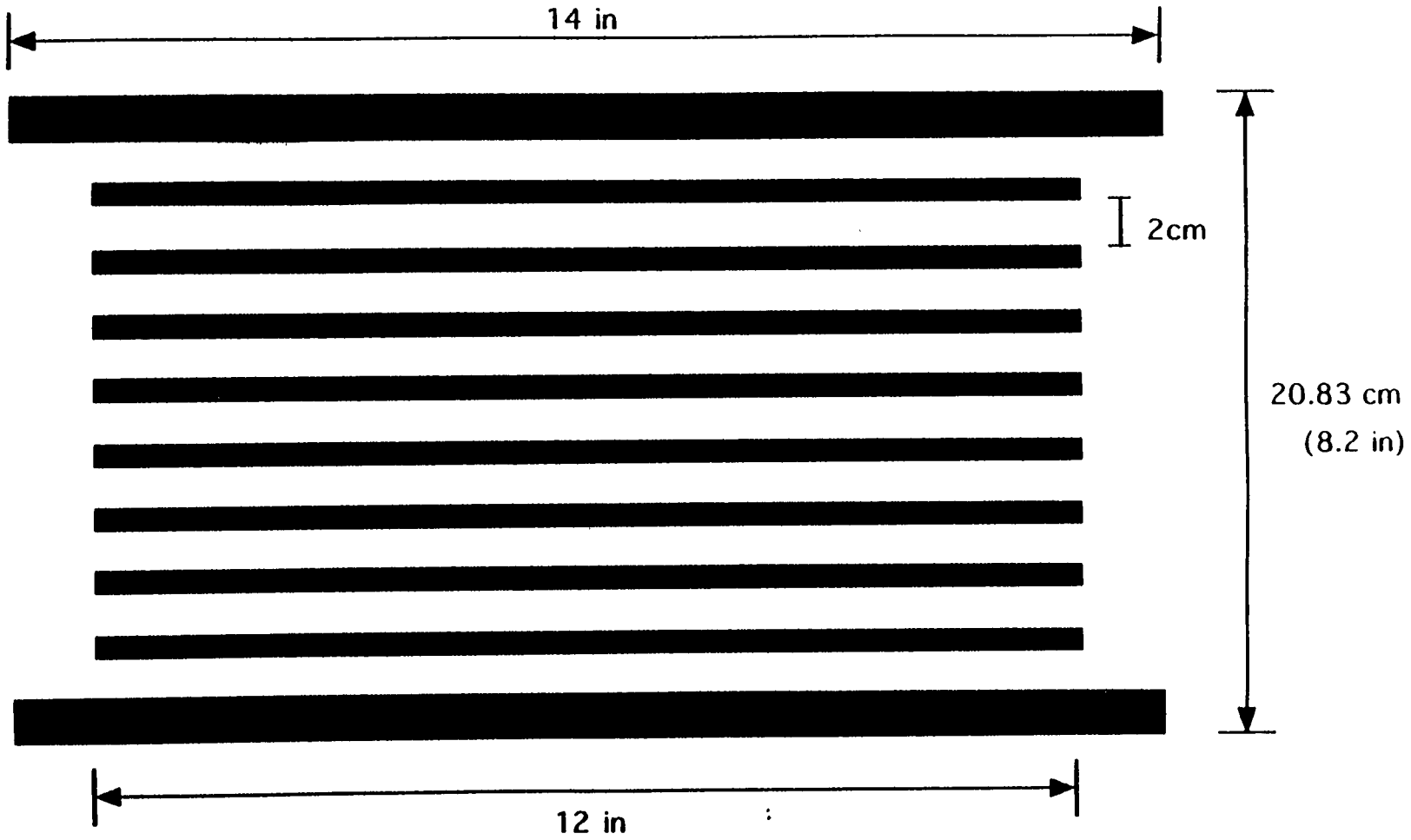

10 Plate Scintillator Stack

1cm thick outer plates
1mm inner plates

Drawing 7.

End View

References

[1]. Omega Engineering, "Measuring Total Air Flow", Omega Flow and Level Handbook vol.28, page C-3. Omega Engineering, 1992

[2]. Russell Gritzo, Malcolm Fowler, and Jan Wouters, "The Development of a Real-Time Monitor for Airborne Alpha Emissions." LA-UR-94-2691.

[3]. Christopher J. Darr, "Background Reduction in the Large Volume Flow Through Detector."

Appendix C

Fluid Flow, Materials, and Structures Research and Development for a Large Volume Flow Detector System.

PRELIMINARY DRAFT

Fluid Flow, Materials, and Structures Research and Development for a Large Volume Flow Detector System

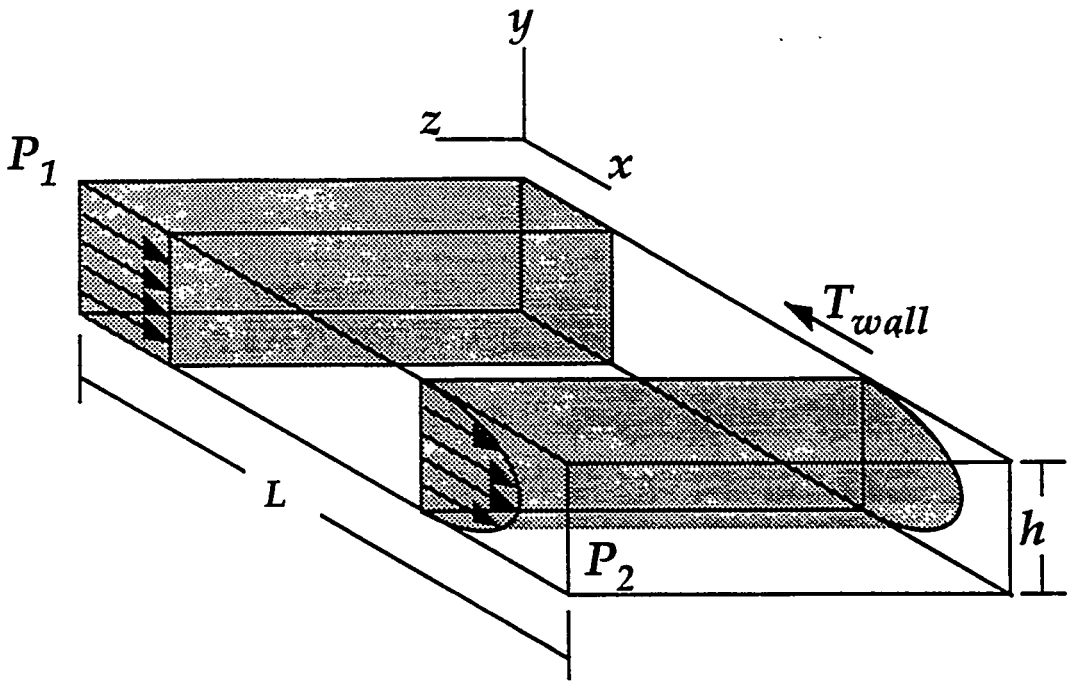

Subject: Fluid Flow Modeling

Principle Investigator: Christopher M. Martinez

Los Alamos
NATIONAL LABORATORY

in collaboration with

Arizona State University
Aerospace Research Center

PRELIMINARY DRAFT

Table of Contents

Introduction

The Large Volume Flow Through Detector System (LVFTDS), currently under development at Los Alamos National Laboratory, is being designed for the real-time detection of alpha particle radiation. Its development is spawned by a growing global environmental concern. As stands, there are a large number of marketable uses for such a detecting system, but the public demands a real-time detection system used for the monitoring of incinerators and other stacks with the potential of emitting alpha particle radiation.

In its incinerator stack working environment, it will act as an alarm which will give split second indications that scrubber and filtration systems have malfunctioned. The detection will allow for the immediate diversion of the exhaust to a possible backup system. Thus preventing the emission of large doses of alpha particle radiation with the potential of causing environmental as well as health threats.

A Large Volume Flow Through Detector System is not a new concept. What makes our LVFTDS unique, as well as useful are its real-time monitoring capabilities. It is this real-time monitoring response that is cause for the prevention of the emission of large doses of radiation into the earth's atmosphere.

A joint effort between Los Alamos National Laboratory and Arizona State University's Aerospace Research Center has been made in order to study the fluid flow, materials, and structural issues affecting the performance of the detecting system. The research necessary for the completion of such a task is the involvement of complex fluid flow models as well as actual tests. These tests range from wind tunnel experiments to PVDF plate physical sensitivities towards practical heat treat temperature variations. The data taken from these various forms of analysis on the system will be used to determine the necessary scope of

mechanical and aerospace development needed to make the system a high performance system.

Los Alamos National laboratory has also given Arizona State University the task of developing an inlet air flow diffuser which will convert a pipe with a circular cross sectional area into a pipe with a rectangular cross-sectional area. The inlet air diffuser will be plugged directly into the inlet of the detector.

The team of researchers and developers at Arizona State University who are working on the project are as follows:

Christopher M. Martinez - Undergraduate Student
Mechanical and Aerospace Engineering

Dr. Helen L. Reed - Director of Aerospace Research Center
Professor, Mechanical and Aerospace Engineering

Dr. William S. Saric - Professor, Mechanical and Aerospace Engineering

Dr. David H. Lannanen - Professor, Mechanical and Aerospace Engineering

Governing Equations

Inlet Reynolds Number

$$Re = \rho V h / \mu$$

Local Reynolds Number

$$Re(x) = \rho V x / \mu$$

Boundary Layer Thickness for Laminar Flow

$$\delta^* = 1.7208 / \ (Re(x))$$

Boundary Layer Thickness for Turbulent Flow

$$\delta^* = 1/8 \ (0.16x/Re\text{^}(1/7))$$

Centerline Local Velocity

$$U_2 = U_1 \ [h / (h - 2\delta^*)$$

Cross Sectional Flow Equation

$$\iint_{cs} \rho\mu \ \vec{v} \bullet \vec{n} \ \ dA$$

Wall Shear for Laminar Flow

$$\tau_{wall} = 0.332 \ \rho^{(1/2)} \mu^{(1/2)} U^{1.5} / x^{(1/2)}$$

Wall Shear Turbulent Flow

$$\tau_{wall} \ \ 0.013 \ \rho^{(6/7)} \mu^{(1/7)} U^{13/7} / x^{(1/7)}$$

Executive Summary

The tasks accomplished throughout the course of the summer of '94 involved a series of simple spreadsheet models as well as complex C language based programs whose jobs were to perform a full scale theoretical analysis of the fluid flow behavior within a detecting cell, as well as the flow's physical influences on the structure of the detector.

Two types of analytical methods were used in the fluid flow analysis; a non-dimensional analysis as well as a dimensional analysis. The non-dimensional analysis was conducted for the purpose of understanding and analyzing fluid flow data within an input range of variables. The dimensional analysis will allow the user to directly input realistic dimensional variables, as a result, the code will give fluid flow characteristics, stresses, strains, and forces acting within, and on the system. The information the code is capable of producing not only describes the scope of the analysis, but also gives us valuable information that not only allows for a scientific statement to be made, but also poses ideas for constructive questions beneficial towards the final structural design of the detecting system.

Leading edges will exist at the inlets of the detecting plates to prevent vortex pockets from forming along the x direction of the fluid flow. Vortex pockets have the potential of obscuring an accurate detection of alpha-particle emission if these pockets were to develop in a real life situation. Vortex pockets would have the tendency to prevent a given number of particles from flowing downstream along x, causing theses particles to repeatedly come in contact with the scintillation plates.

The preliminary structures and materials tests will deal with several stretch techniques in an attempt to define the scintillation material's modulus of elasticity and density, Allowing us to choose a material with the same kinds of physical characteristics. Once this mock material has been determined, it will be used to mock up the scintillation plates in the wind

tunnel models. To ensure accurate heat treat data, samples of the PVDF scintillation material will be used in the ovens. Question: Will the plates lose their detection accuracy after they've been exposed to their working environmental temperatures? The heat treat results as far as the physical aspects are concerned will help determine what kinds of structural measures will have to be taken in order to ensure the detector's capability of withstanding those short and long term affects that it will be exposed to by its environmental working elements.

Several possible creative ideation designs have been developed for an airflow inlet diffuser. Due to cost considerations and theoretical assumptions, one inlet diffuser design assumed to be the best design for its given function has been chosen. This inlet diffuser design will not be finalized until the design is wind tunnel tested. Wind tunnel tests will probably lead to the diffusers modification. The diffuser is being designed to equally disperse fluid volume to the inlets of each detecting cell.

Acknowledgments

I would like to thank Dr. Helen L. Reed for advising and challenging me, and offering her unending support in working on the LVFTDS. I would also like to thank the ERC 315 crew for their support, encouragement, and technical help. The project, for the most part, is coming to a theoretical close, and entering its experimental and developmental stages. The project is still quite young and I am looking forward to working with Dr. David H. Lannenen and Dr. William S. Saric whom I would also like to thank for their interests in the project.

I would like to thank Jody Heiken, and Ward Zealke for their support as well as Russ Gritzo and Malcom Fowler for allowing me the opportunity to work on the project.

Non - Dimensional Analysis

The non-dimensional analysis conducted on the fluid flow within a detecting cell was done using the Eulerian method. Therefore, concern is dealt with the properties of the flow as the flow enters and leaves the system. The analysis provides fluid flow characteristics for any scenario cared to be investigated. The code used to calculate the fluid flow for the non-dimensional analysis is a variable range driven program. It allows the user to investigate the fluid flow properties within the cell at a range of practical input variables.

The input variables are listed as follows:

Detector cell length along x direction of fluid flow
Temperature (Ambient)
Pressure (Ambient)
Initial fluid flow velocity
Plate space width
Number of intervals along x
Number of Reynolds numbers

Temperature is used to compute viscosity with the use of the Sutherland formula, and both pressure and temperature are used to compute fluid density using the ideal gas law. Once this process had taken place, all the dimensional variables needed for further calculation are preprocessed into non-dimensionalizing parameters using the Buckingham PI Theorem. These non-dimensional parameters are then configured into ratios named alpha, beta, and gamma.

(A copy non-dimensionalized code can be found in Appendix A-1.)

These ratios are directly proportional to the following:

alpha - distance from the inlet in the positive x-axis direction
beta - centerline local velocity
gamma - boundary layer thickness

These ratios are calculated locally at a user input number of progressive lengths in the positive x direction.

Analysis of the Results

After analyzing the results shown in the plots in Appendix C thru Appendix F, it can be noted that the fluid flow at the inlet of the detecting cell is laminar, this is represented by the first curve beginning at the inlet of the x distance. As the flow progresses down the x-axis, it goes from a laminar flow, to a transition flow, and finally a turbulent flow. This transition of flows is clearly evident in the velocity and boundary layer plots seen as a sudden irregularity in their curves. A visual representation of these flows are illustrated in the photo below.

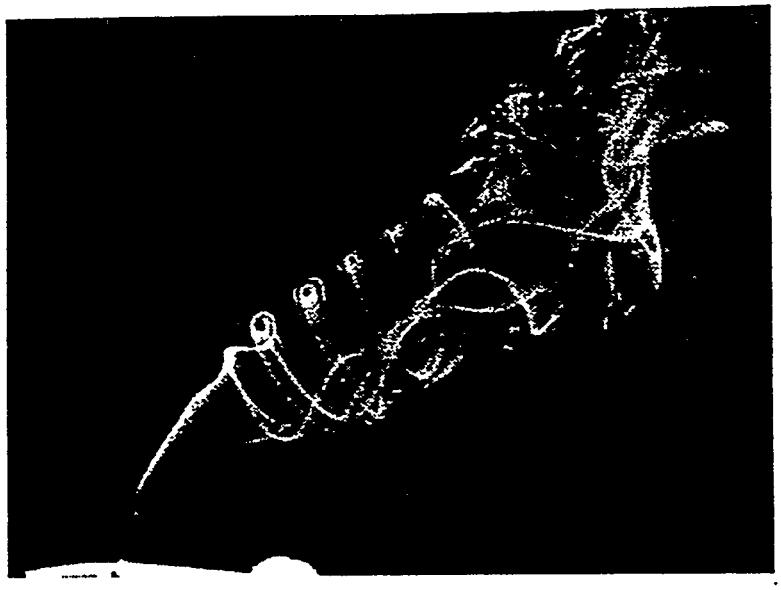

The existing changes in local centerline velocity show an existence of acceleration. This is a resultant of the fluid's viscous effects that are caused by a wall shear applied to the fluid by the detecting plates. This is proof that laminar as well as turbulent flow will cause air to come into contact with the plates, thus bringing the alpha particles in contact with the detecting plates.

In laminar flow, the only alpha particles that will come into contact with the detecting plates are those that are flowing through the streaklines that make contact with the scintillation plates.

In turbulent flow, an assumed majority of alpha particles within the volume of a detecting cell will come into contact with the detecting plates.

The length along x at which laminar flow goes into transition is known as the flow's entrance length, transition occurs at a local Reynolds number of 250,000. Fluctuations in Reynolds numbers will cause the flow's entrance length to fluctuate. This fluctuation can cause fluctuating discrepancies in error when compared to a calculated ideal alpha particle detection reading. This is due to the fact that a higher percentage of alpha particles come in contact with the detecting plates in turbulent flow when as compared to the percentage of particles that come in contact with the detecting plates while in laminar flow. Two practical entrance length sensitivity plots were generated as functions of temperature fluctuation as well as fluid flow inlet velocity fluctuations. These plots show a reasonably small change in entrance length. The only drawback is the fact that temperature and air-flow velocities will have to be carefully monitored and controlled.

To eliminate this problem, the inlet air diffuser has been designed to induce turbulence at the inlet of the detecting system, thus eliminating the total presence of laminar flow. This is done by adding sufficient length to the diffuser so as to increase the local Reynolds number downstream, this high Reynolds number will represent turbulence at the inlet of the detector. To aid in the flow's transition to turbulence, a screen may be placed at the inlet of the air flow diffuser. A screen has the tendency of causing transition.

Blunt leading edges will prevent vortex pockets over the plates from forming.

Case studies using the dimensionalized code show a trivial amount of stress and strain applied to each plate. At room temperature the detector should have no structural problems posed as a cause of fluid flow.

Figure 1-1

Ideation Drawing for an Inlet Air Diffuser

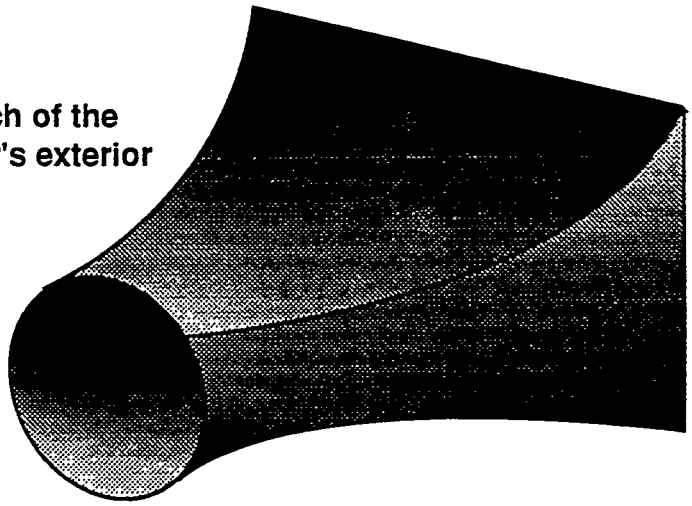

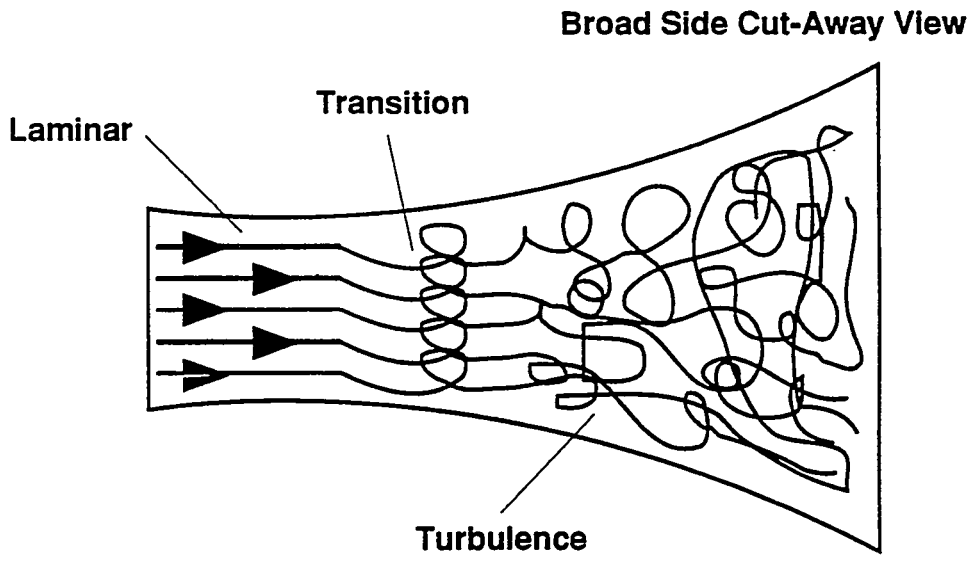

The purpose of this diffuser is to be able to induce turbulent flow as well as equal volumes of air flow into each detecting cell. It is assumed that this can be achieved simply by optimizing an extented diffuser length. This assumption will be tested in a flow visualization wind tunnel. Other possible modifications to this design will be disscussed in the following pages.

Appendix A

Fluid Flow Code in C Language (Dimensional and Non-Dimensional)

Note: This section omitted for brevity. A copy of this section is available from R. Gritzo upon request.

Appendix B
Example of Results from the Dimensionalized Code

Note: This section omitted for brevity. A copy of this section is available from R. Gritzo upon request.

Appendix C
Fluid Flow Plots Corresponding for a Set of all Practical Variable Scenarios

Variables:

Cell length along x = 1 ft
Temperature range = 45 - 90 Deg. C
Pressure = 1 - 5 atm
Inlet Velocity = 4.470278 - 44.70278 m/s
Plate Space Width = 2 cm
Number of Reynolds numbers = 20
Number of alphas = 100

(2D) || Print || 25 Sep 1994 || flow1.plt ||

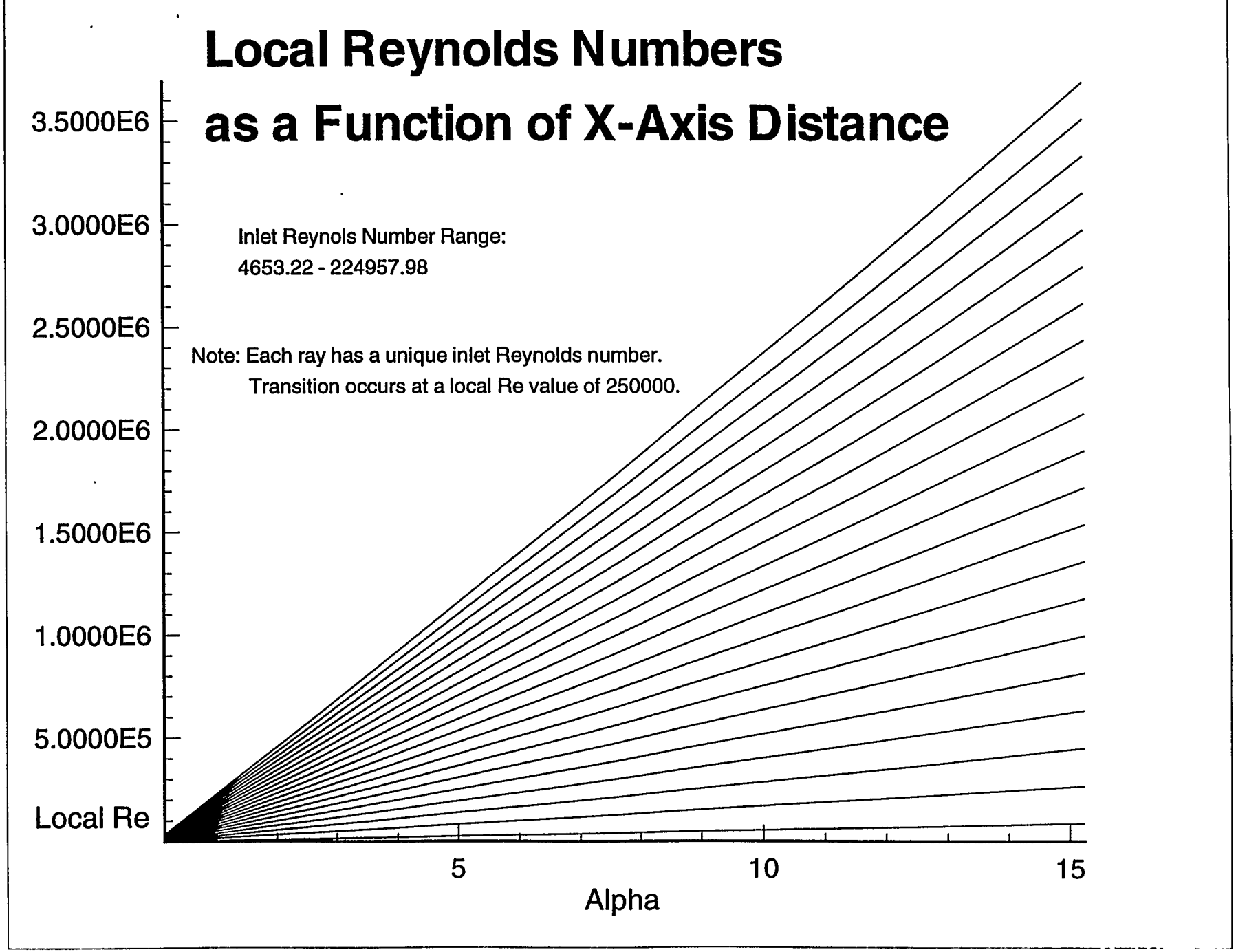

(2D) || Print || 25 Sep 1994 || flow1.plt ||

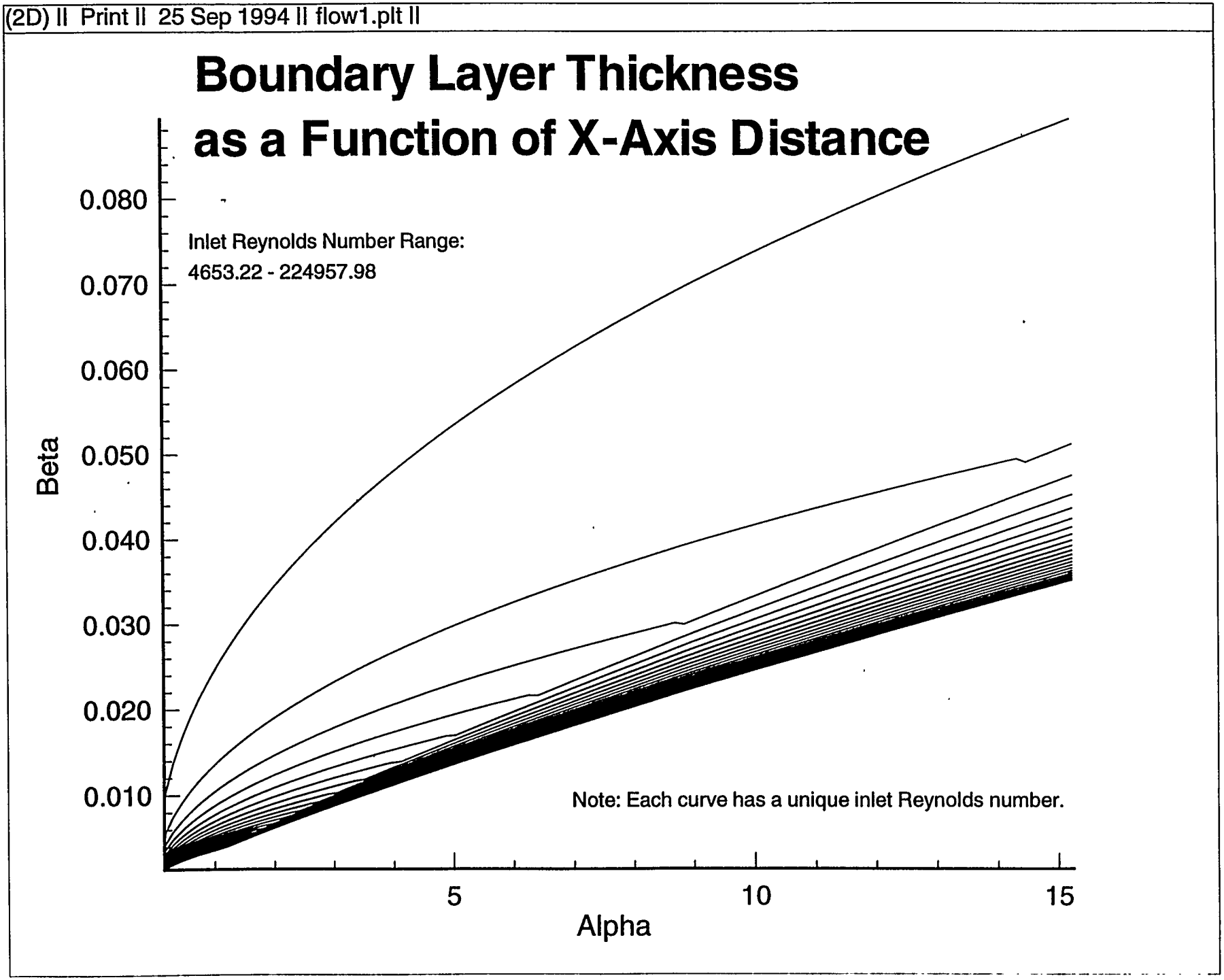

(2D) || Print || 25 Sep 1994 || flow1.plt ||

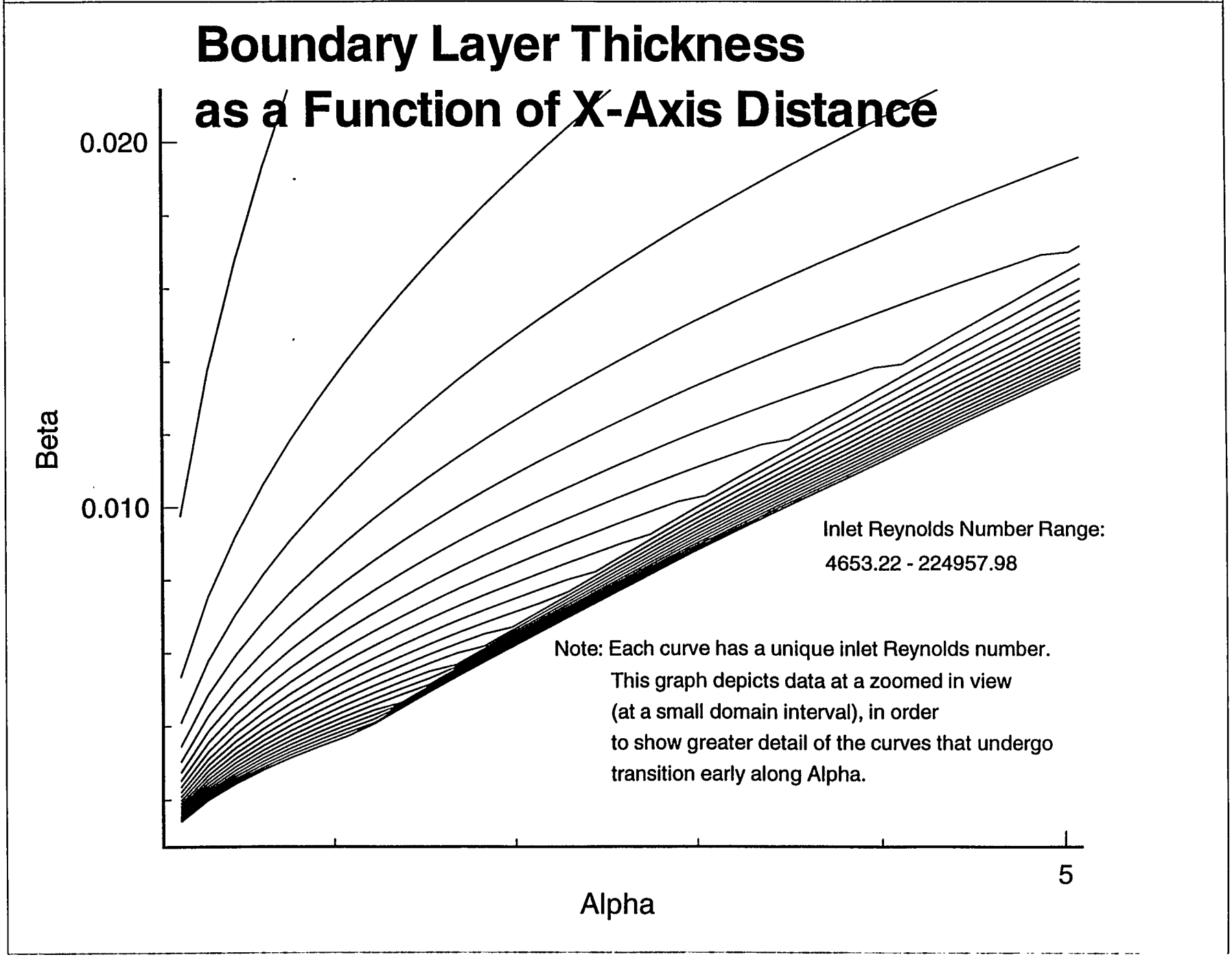

(2D) || Print || 28 Sep 1994 || flow1.plt ||

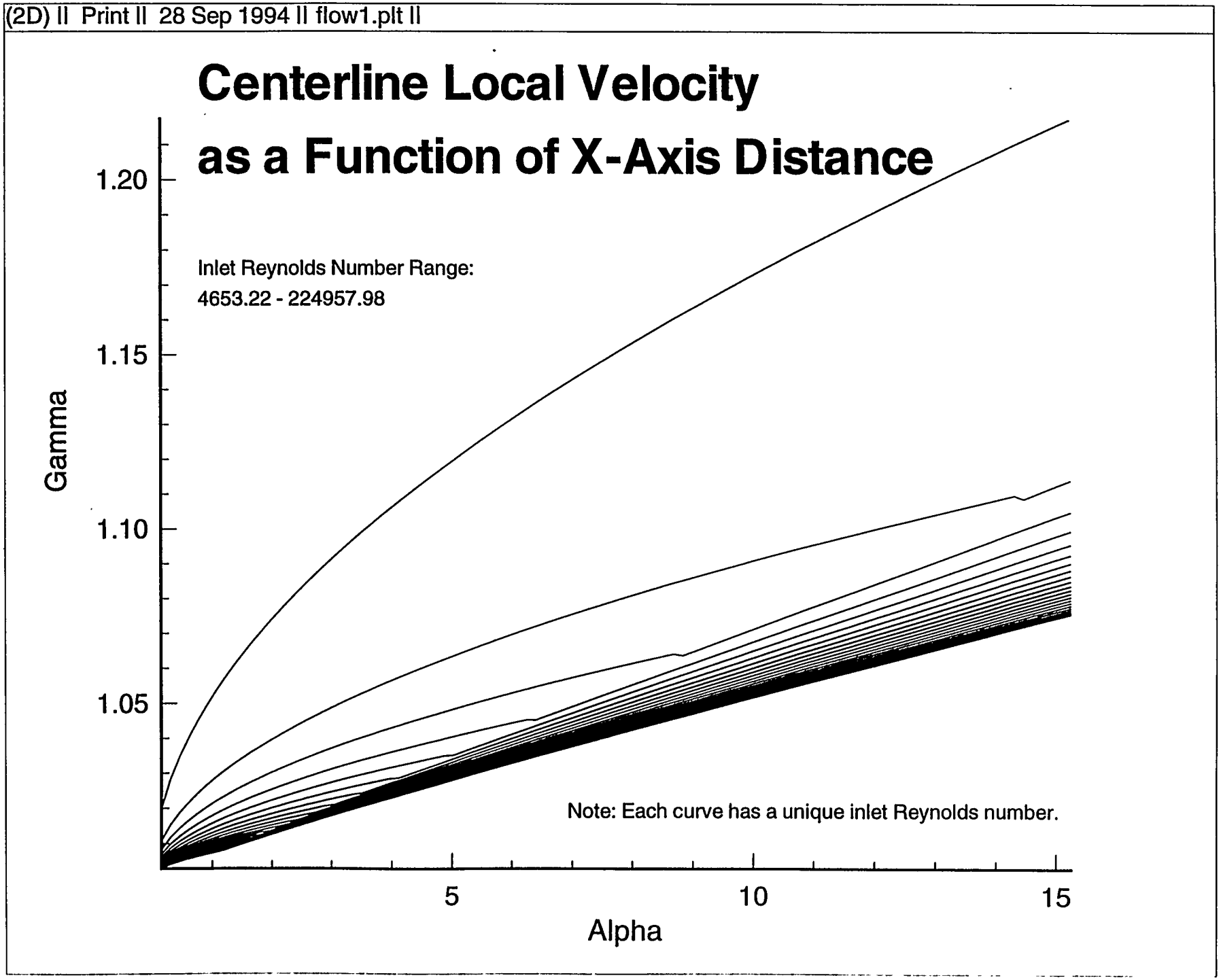

(2D) || Print || 28 Sep 1994 || flow1.plt ||

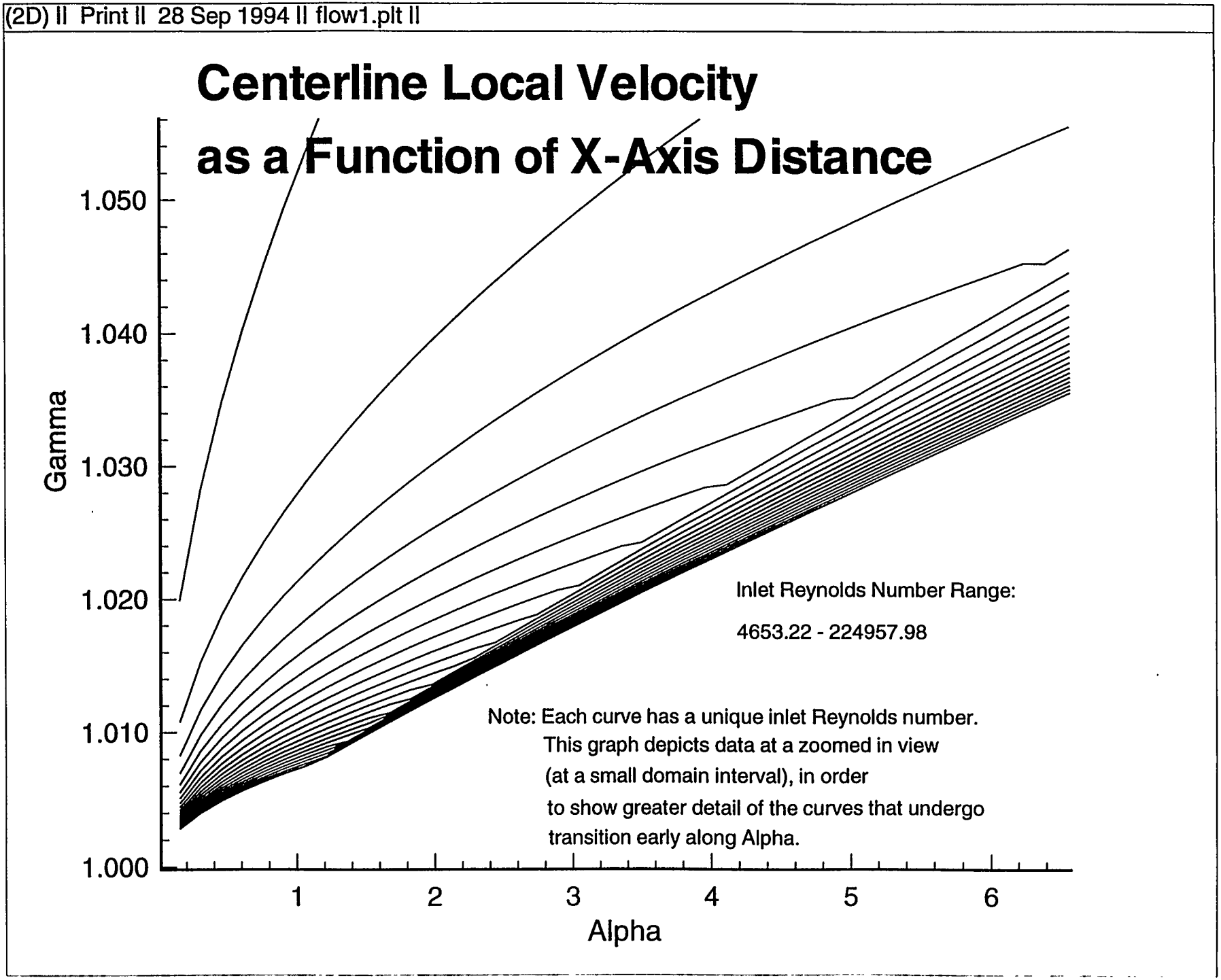

Appendix D
Realistic Fluid Plots Corresponding for a Set of all Practical Variable Scenarios

Variables:

Cell length along x = 1 ft
Temperature range = 60 - 90 Deg. C
Pressure = 1 - 3 atm
Inlet Velocity = 26.82167 - 44.70278 m/s
Plate Space Width = 2 cm
Number of Reynolds numbers = 20
Number of alphas = 100

(2D) II Print II 25 Sep 1994 II flow2.plt II

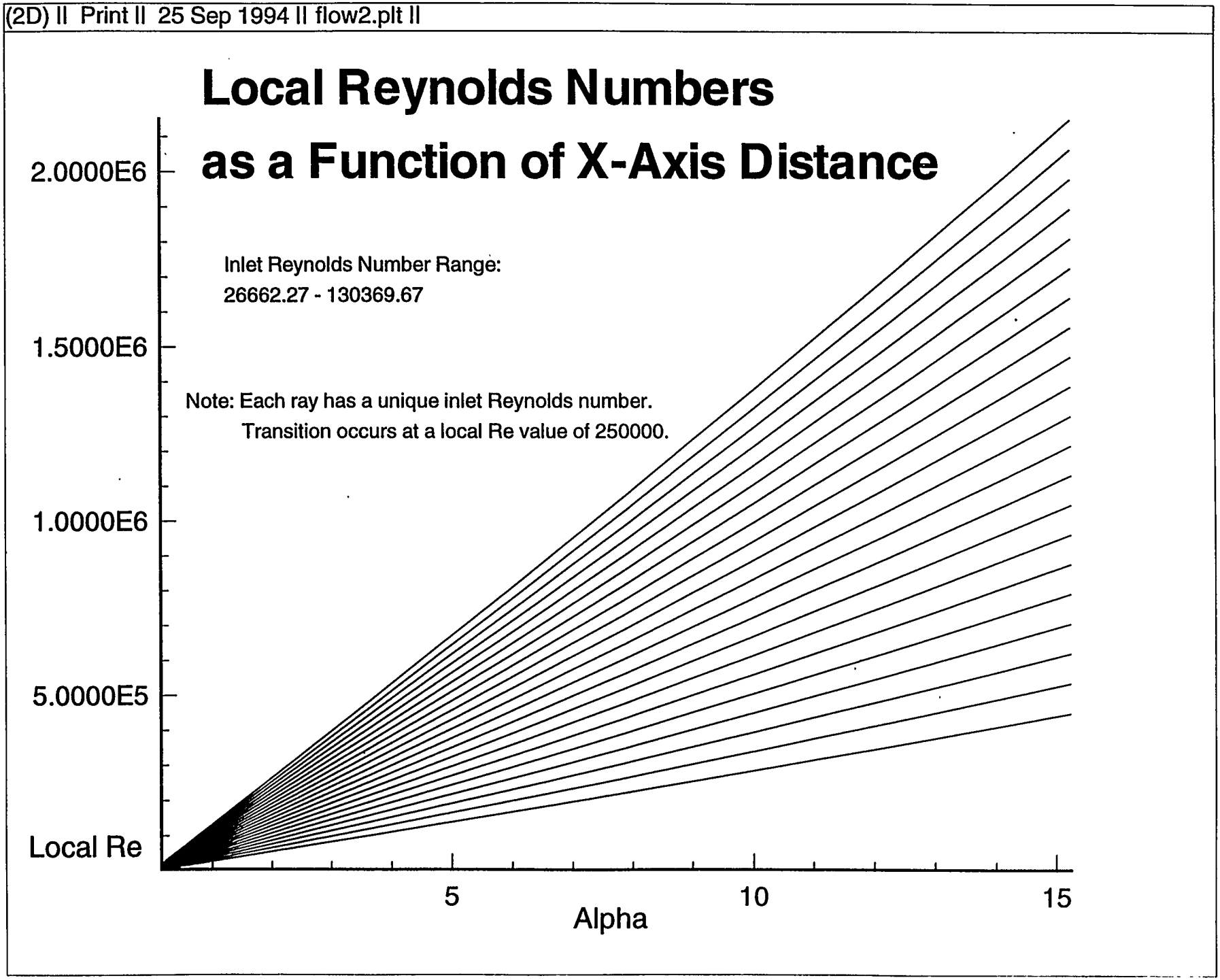

(2D) || Print || 25 Sep 1994 || flow2.plt ||

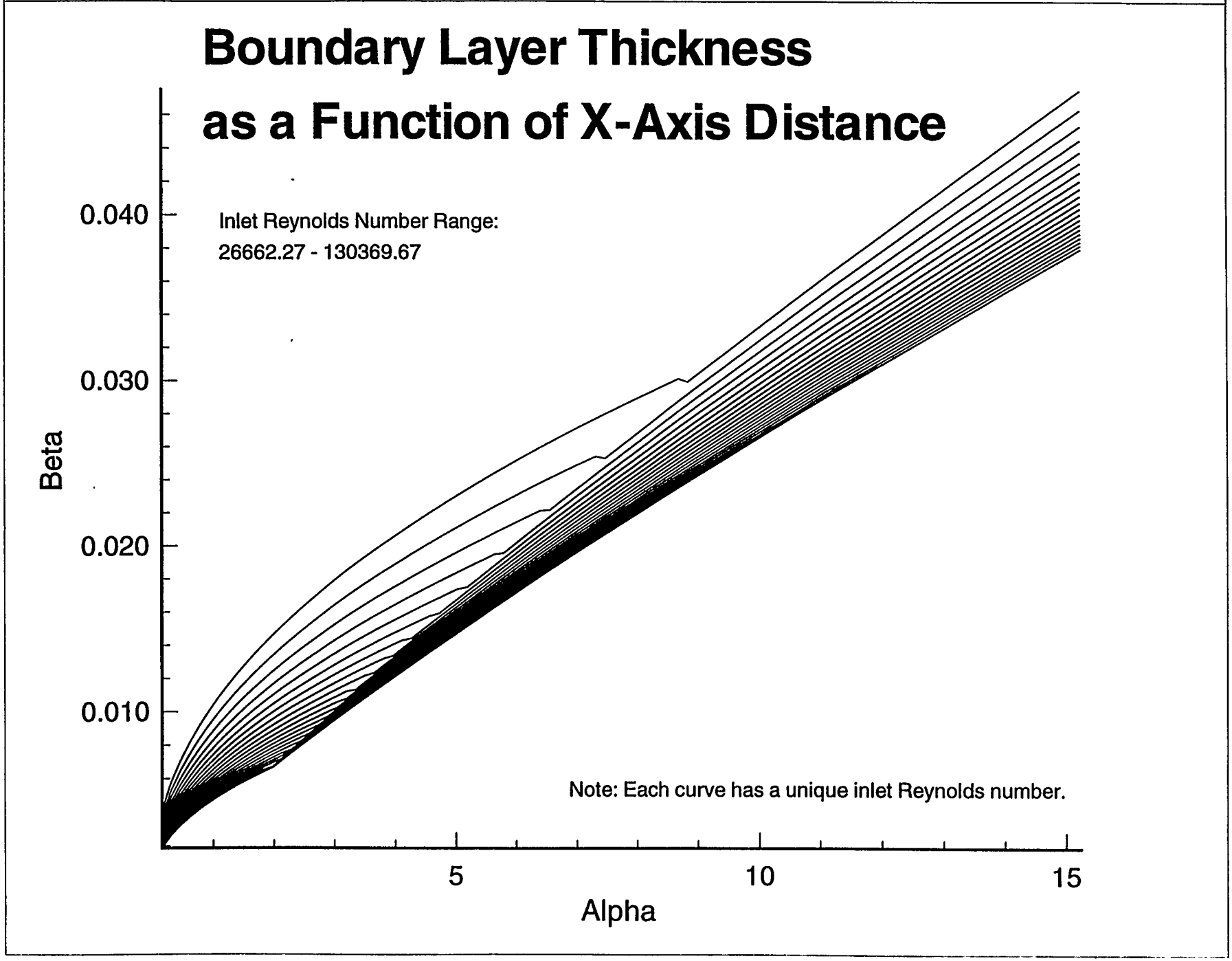

(2D) || Print || 25 Sep 1994 || flow2.plt ||

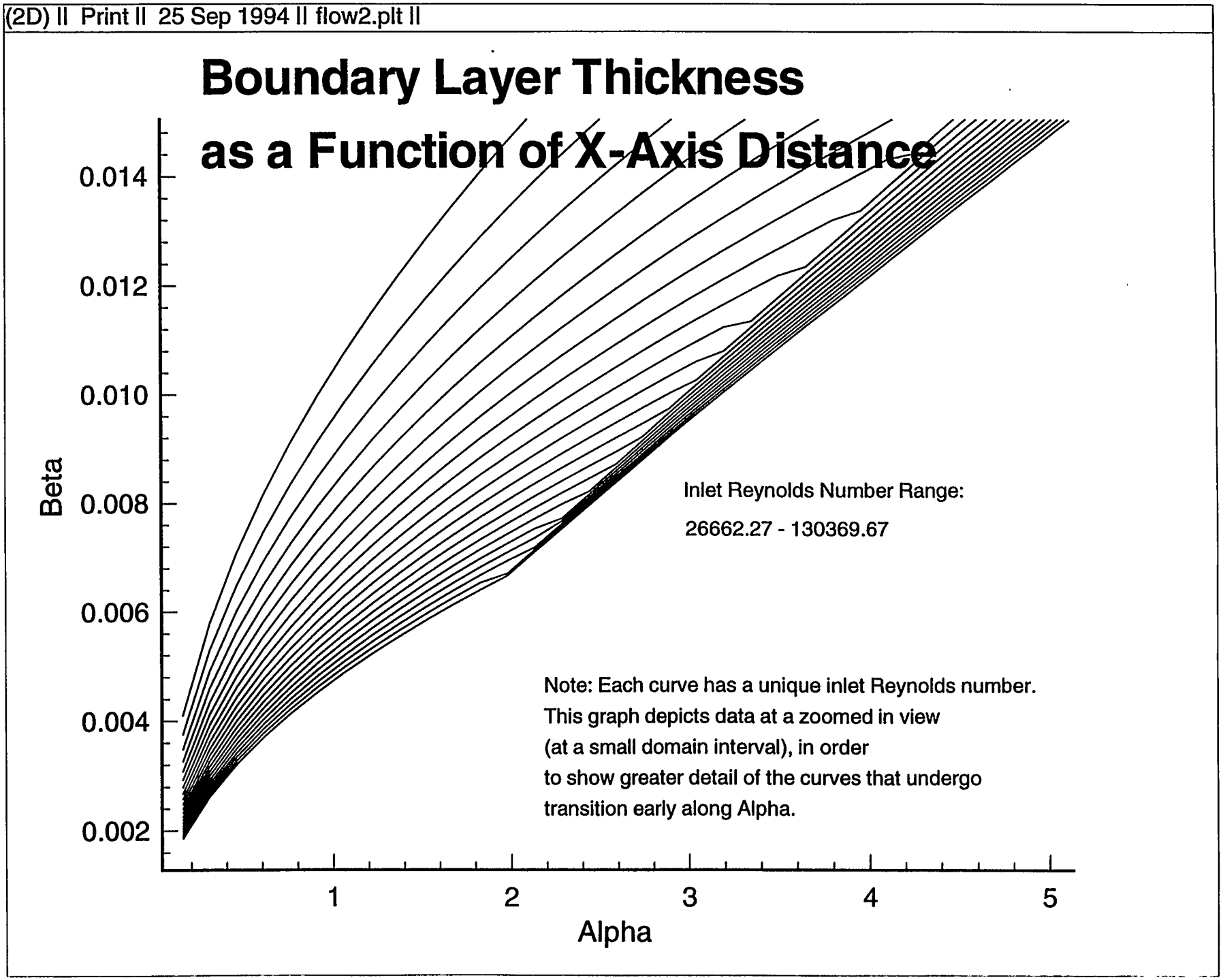

(2D) || Print || 28 Sep 1994 || flow2.plt ||

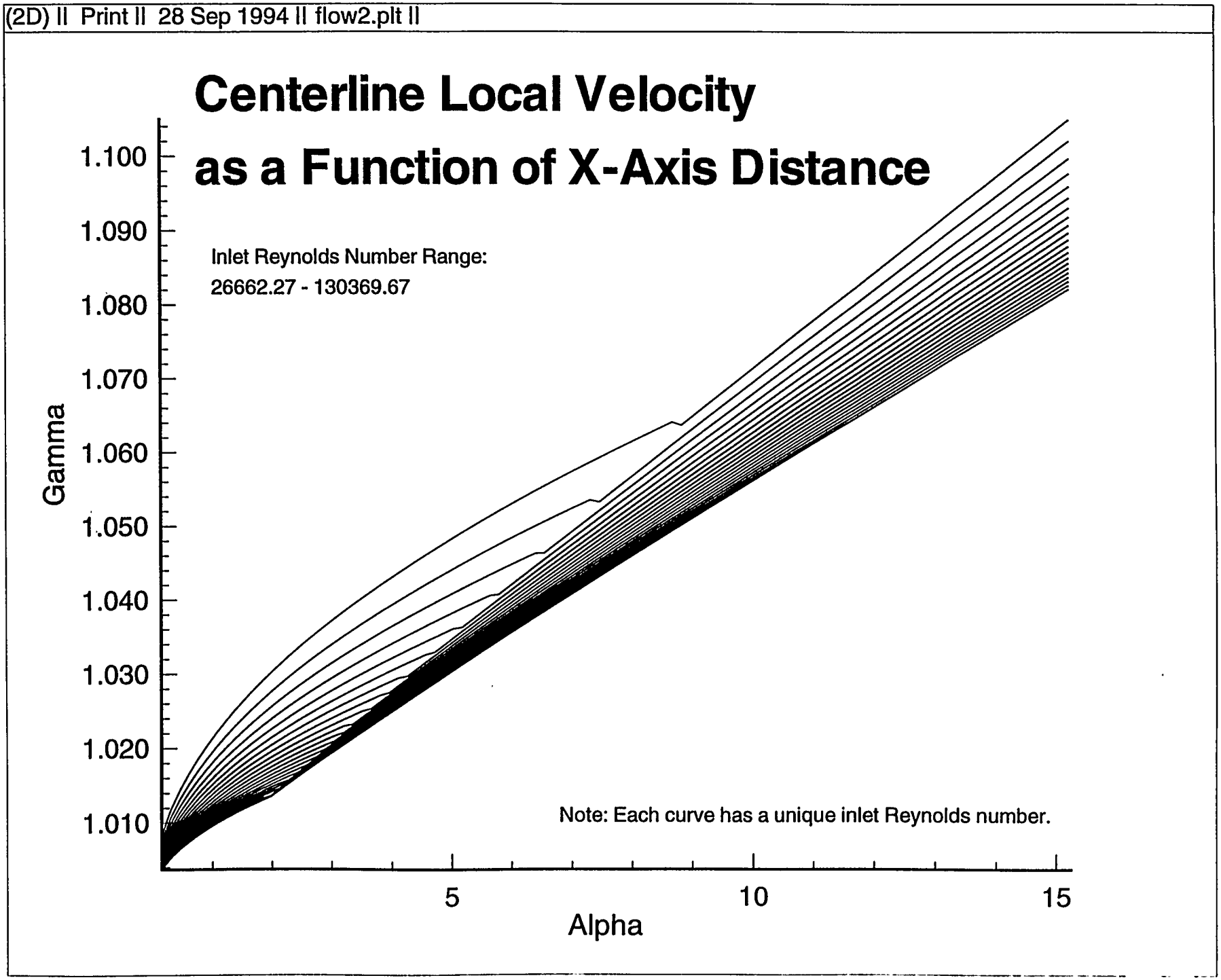

(2D) || Print || 28 Sep 1994 || flow2.plt ||

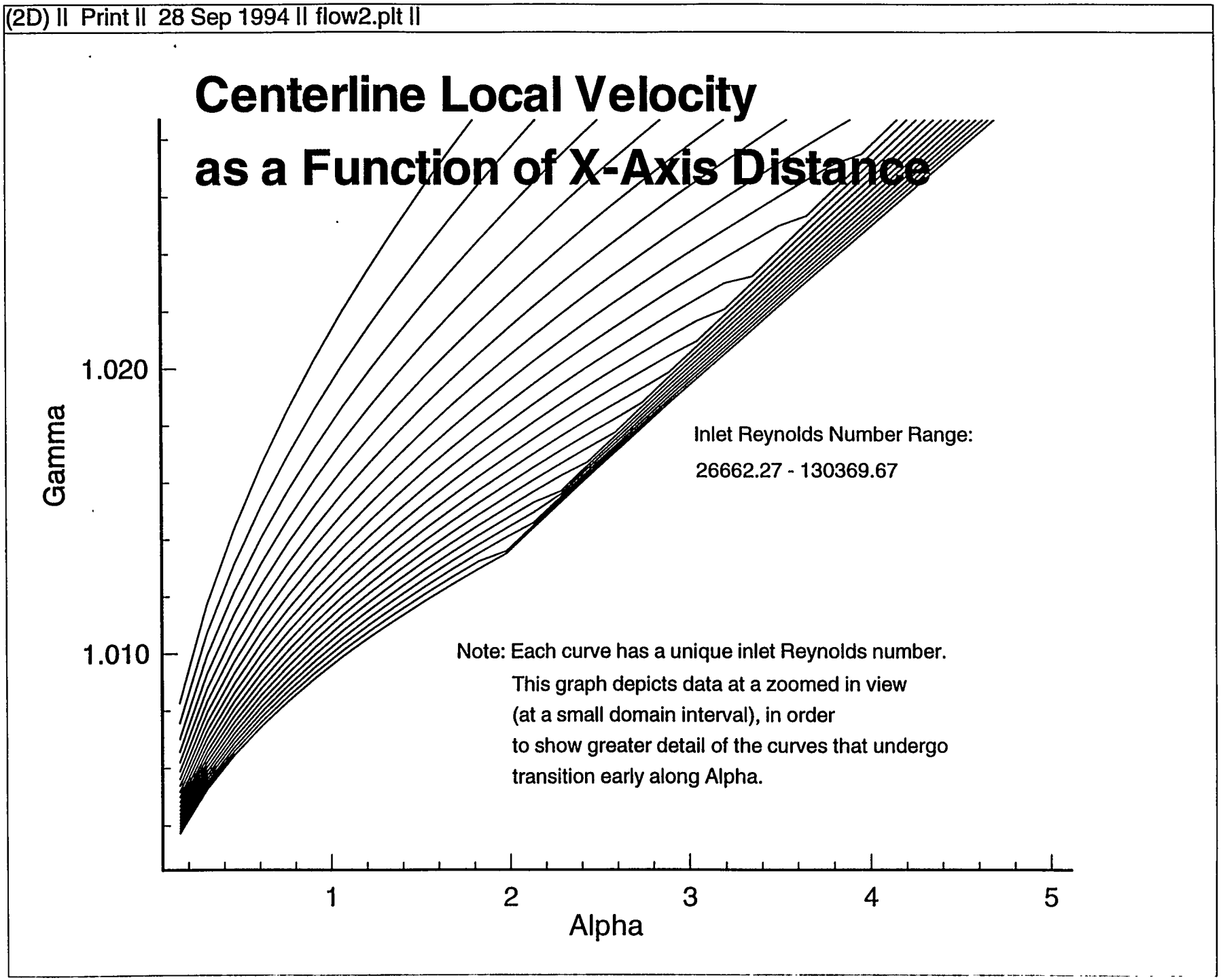

Appendix E
Realistic Inlet Velocity Sensitivity Plot

Variables:

Cell length along x = 1 ft
Temperature range = 75.5 - 75.5 Deg. C
Pressure = 1 - 1 atm
Inlet Velocity = 30.00 - 50.00 m/s
Plate Space Width = 2 cm
Number of Reynolds numbers = 20
Number of alphas = 100

(2D) || Print || 26 Sep 1994 || flow3.plt ||

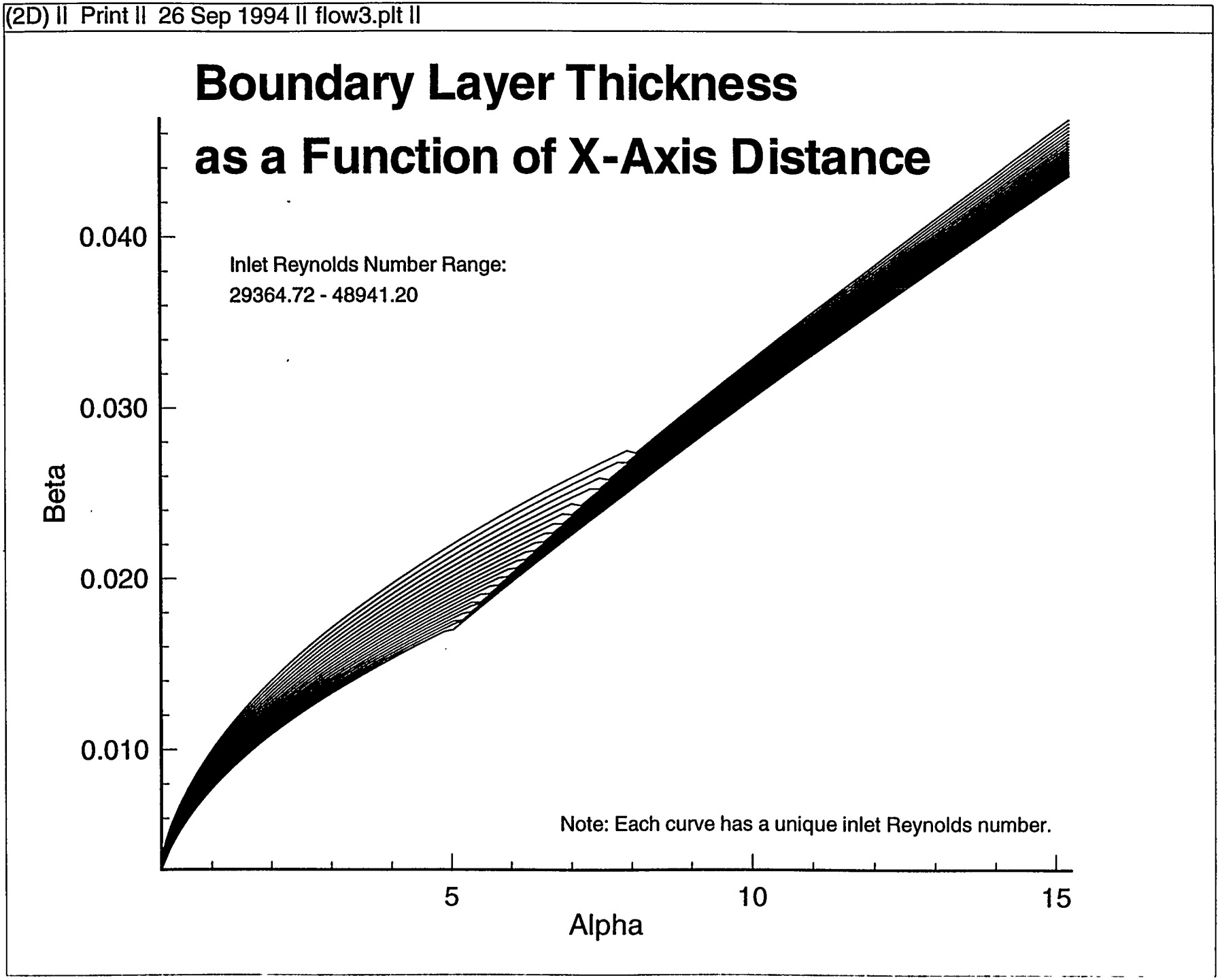

Appendix E
Realistic Temperature Sensitivity Plot

Variables:

Cell length along x = 1 ft
Temperature range = 65 - 90 Deg. C
Pressure = 1 - 1 atm
Inlet Velocity = 40.232502 - 40.232502 m/s
Plate Space Width = 2 cm
Number of Reynolds numbers = 20
Number of alphas = 100

(2D) || Print || 26 Sep 1994 || flow4.plt ||

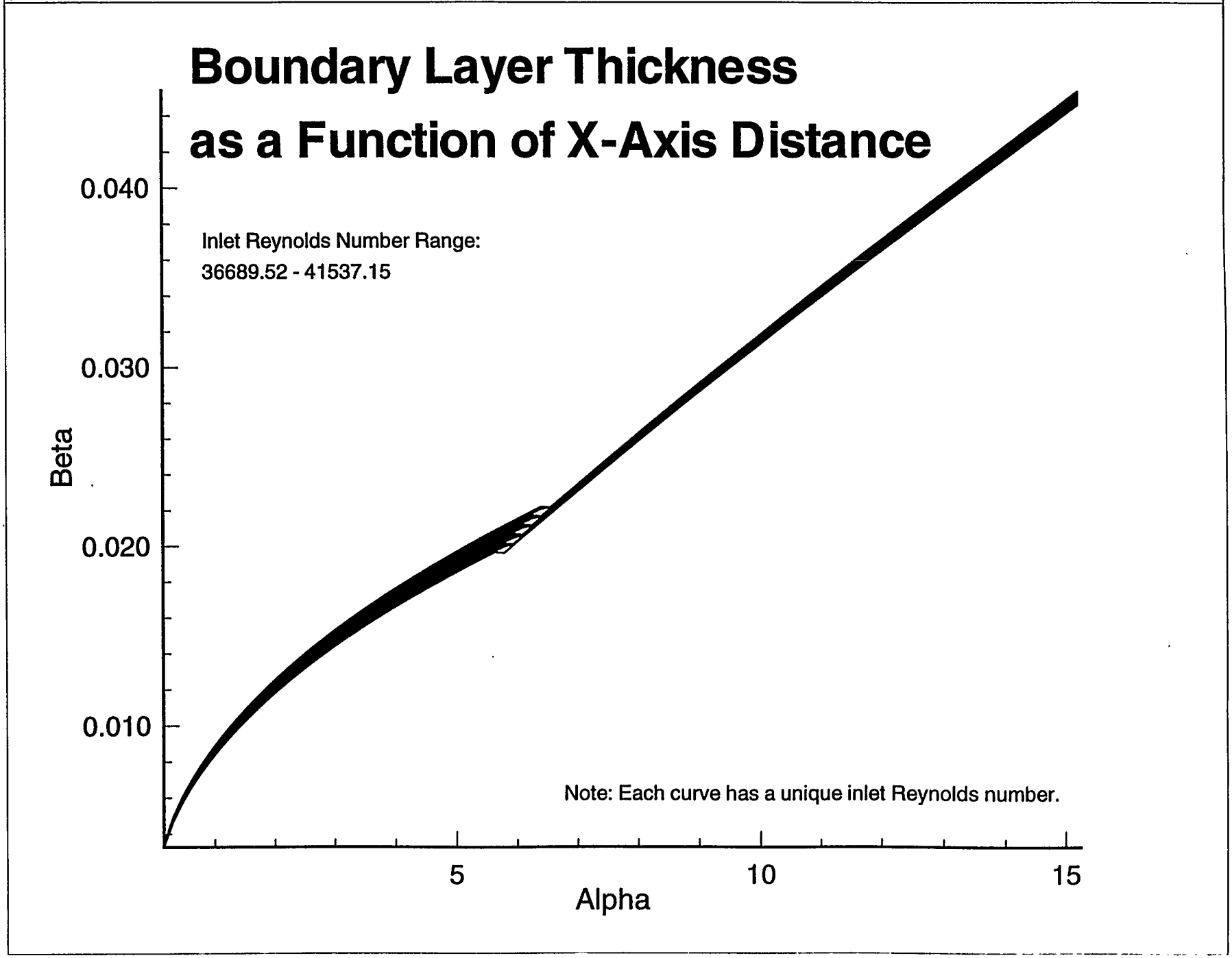

(2D) || Print || 26 Sep 1994 || flow4.plt ||

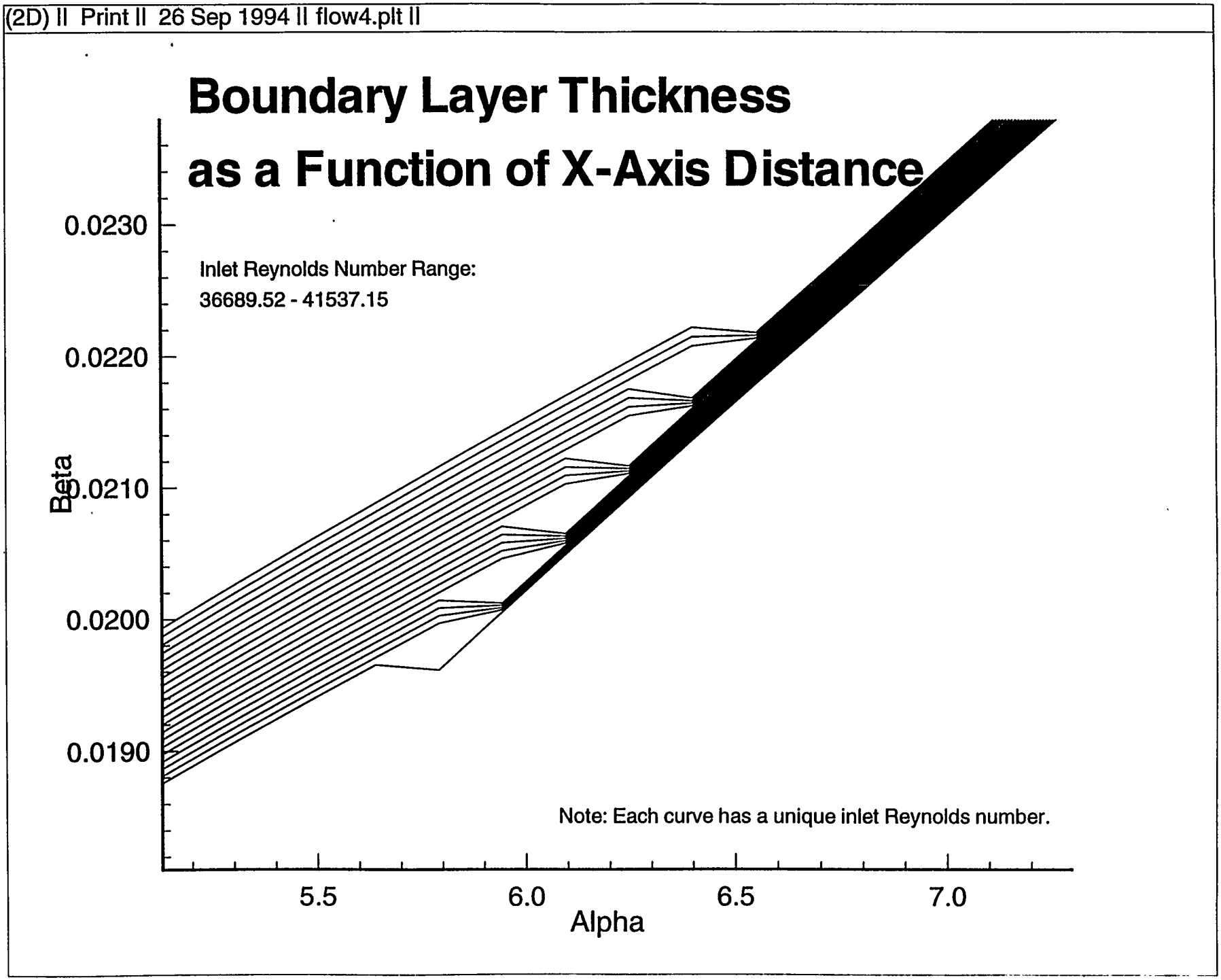

References

An Album of Fluid Motion, Assembled by Van Dyke:

Dept. of Mechenical Engineering, Stanford University. 1992

(For photograph of Laminar-Transition-Turbulence)